ISTANBUL TECHNICAL UNIVERSITY ★ GRADUATE SCHOOL OF SCIENCE ENGINEERING AND TECHNOLOGY

DESIGN AND CONSTRUCTION OF A SETUP FOR THE DETECTION OF TUNNELING INDUCED PHOTONS IN A SCANNING TUNNELING MICROSCOPE AND AN APPLICATION ON GOLD SURFACES

M.Sc. THESIS

Mehmet Selman TAMER

Department of Physics Engineering

Physics Engineering Programme

JANUARY 2013

ISTANBUL TECHNICAL UNIVERSITY ★ GRADUATE SCHOOL OF SCIENCE ENGINEERING AND TECHNOLOGY

DESIGN AND CONSTRUCTION OF A SETUP FOR THE DETECTION OF TUNNELING INDUCED PHOTONS IN A SCANNING TUNNELING MICROSCOPE AND AN APPLICATION ON GOLD SURFACES

M.Sc. THESIS

Mehmet Selman TAMER
(509091126)

Department of Physics Engineering

Physics Engineering Programme

Thesis Advisor: Assoc. Prof. Dr. Oğuzhan GÜRLÜ

JANUARY 2013

İSTANBUL TEKNİK ÜNİVERSİTESİ ★ FEN BİLİMLERİ ENSTİTÜSÜ

TARAMALI TÜNELLEME MİKROSKOBUNDA TÜNELLEME İLE UYARILMIŞ PHOTONLARIN GÖZLEMLENMESİ İÇİN SİSTEM TASARLANMASI VE KURULUMU VE ALTIN YÜZEYLERİNDE UYGULANMASI

YÜKSEK LİSANS TEZİ

Mehmet Selman TAMER
(509091126)

Fizik Mühendisliği Anabilim Dalı

Fizik Mühendisliği Programı

Tez Danışmanı: Doç. Dr. Oğuzhan GÜRLÜ

OCAK 2013

Mehmet Selman TAMER, a **M.Sc.** student of ITU **Graduate School of Science and Engineering** student ID **509091126**, successfully defended the **thesis** entitled "Design and construction of a setup for the detection of tunneling induced photons in a scanning tunneling microscope and an application on gold surfaces", which he prepared after fulfilling the requirements specified in the associated legislations, before the jury whose signatures are below.

Thesis Advisor : **Assoc. Prof. Dr. Oğuzhan GÜRLÜ** ....
İstanbul Technical University

Jury Members : **Assoc. Prof. Dr. Sevtap ÖZBEK** ....
İstanbul Technical University

Prof. Dr. Mustafa ÜRGEN ....
İstanbul Technical University

Date of Submission : 17 DEC 2012
Date of Defense : 25 JAN 2013

To my FAMILY,

FOREWORD

Life in Turkey is just like the climates in Turkey. It can be winter, autumn, summer or spring. That is why we do not have stable life or stable relations with people. It can be rainy, stormy, sunny or hot, but after all we are a great country with great people and we have many different fruits at every different climate. This is the summary of my story in İstanbul Technical University with my advisor Oguzhan Gürlü and laboratory. We lived many different climates and we had many different fruits at all time. I hope the end of my story for master degree will not be the end of our story with him. I would like to thank him for everything he did for me.

I would like to thank Ümit Çelik, Tansu Ersoy, and members of surface physics research laboratory for their friendship and support to this work and me.

I feel myself very lucky to have so many wonderful friends to greatfuly thank for their friendship. I would like to thank Ahmet Yağmur, Ferhat Özduran, Hüseyin Ikizler, Mehmet Sayın, Mustafa Emin, and Yusuf Ekrem Eren for obstructing my research with their friendship and with their uninvited visits.

For sure, the most important part of the research is budget. I would like to thank Türkiye Bilimsel ve Teknolojik Araştırma Kurumu, TUBITAK for their support for this research (Project No: 109T687).

I would like to thank Merve Altay for being my soul mate, supporter, lover,friend and everything.

My brothers Furkan, Hüseyin, Osman, Eyüp, my sisters Sümeyye and Sinem and of course my father Şükrü and my mother Ayşe had great support on me. I would like to thank to them for their great supports and love.

December 2012 Mehmet Selman TAMER

TABLE OF CONTENTS

Page

ABBREVIATIONS

SPM : Scanning Probe Microscopy
SPI : Scanning Probe Instruments
STM : Scanning Tunneling Microscopy
TTM : Taramalı Tünelleme Mikroskopu
PESTM : Photon Emission from Scanning Tunneling Microscope
DOS : Density Of States
LDOS : Local Density Of States
OpAmp : Operational Amplifier
HOPG : Highly Oriented Pyrolytic Graphite
ML : Monolayer
CAD : Computer Aided Design
AC : Accelerating Current
DC : Direct Current
PMT : Photomultiplier Tube
AFM : Atomic Force Microscope

LIST OF TABLES

Page

LIST OF FIGURES

Page

DESIGN AND CONSTRUCTION OF A SETUP FOR THE DETECTION OF TUNNELING INDUCED PHOTONS IN A SCANNING TUNNELING MICROSCOPE AND AN APPLICATION ON GOLD SURFACES

SUMMARY

Understanding the electronic and optical properties in atomic and molecular scale is a great challenge to deal with. Imaging and analyzing materials in this scale size had been the main motivation for development of different variety of microscopy and spectroscopy techniques.

In 1986, Gerd Binnig and Heinrich Rohrer reported the first successful tunneling experiment, the Scanning Tunneling Microscope (STM). STM was leading the surface science studies to more interesting and more challenging areas with tunneling electrons.

STM is used to visualize the surface topography of conducting and semiconducting materials in atomic scale with 0.01 nm resolution. In addition to that STM made many spectroscopic techniques possible for single particles in atomic scale, stimulated by tunneling electrons.

After the invention of STM, Gimzewski et al. reported the photon emission from STM stimulated by tunneling electrons. The photon emission from STM at atomic resolution has proven that the resolution limits for this spectroscopy technique could be as high as the imaging limits of STM.

Introduction of photon emission from STM created new opportunities to study the electronic and optical properties of the nanostructures such as nano-wire, quantum wells or quantum dots etc. STM is not only used to image nanostructures on metal surface, but also STM makes it possible to investigate the energy spectrum of nanoparticles between metal surface and metal tip.

Nano structures, such as quantum dots, show quantum physical properties rather than classical properties. The effects of quantum confinement create differences between the bulk material semiconductors and nanostructured semiconductors in manner of electronic and optical properties. Another important area to study with STM is; it is possible to excite surface plasmons locally between tip and sample. Studies on surface plasmons are very important for nano photonics.

In this thesis, a development of experimental setup for observation of photon emission from scanning tunneling microscope and application results on rough Au surface will be presented. Surface plasmons are located on the surface of a conducting sample surface and photon emission is induced by tunneling electrons between tip and sample. The physical background for photon emission from scanning tunneling microscope, development of experimental setup for photon emission measurements from scanning tunneling microscope, our results, discussions about the results and expected future works will be explained respectively.

TARAMALI TÜNELLEME MİKROSKOBUNDA TÜNELLEME İLE UYARILMIŞ PHOTONLARIN GÖZLEMLENMESİ İÇİN SİSTEM TASARLANMASI VE KURULUMU VE ALTIN YÜZEYLERİNDE UYGULANMASI

ÖZET

Malzemenin özelliği, nanometre mertebesi gibi küçük boyutlara inildikçe, büyük boyutlarda gösterdiği özelliklerden çok daha farklılıklar göstermeye başlar. Bu boyutlarda malzemeyle çalışmak oldukça zor ve anlaşılması zordur. Taramalı uç mikroskopisinde gelinen nokta bu alanda çalışmak isteyenler için oldukça ümit verici olmuştur.

Taramalı uç mikroskoplarının bize sağladığı 0.01nm çözünürlükte görüntüleme kapasitesine sahip olan taramalı tünellemeli mikroskopisi bu alanda önemli bir yere sahiptir. TTM ile iletken ve yarı iletken yüzeylerde yüzey topografyasını çıkarmakla kalmaz bize aynı zamanda tünelleyen elektronlarla yüzey üzerinde spektroskopik ölçümler almamıza olanak sağlar.

TTM bize aynı zamanda tünelleyen elektronların yarattıkları etkiler ile ilgili çalışmamıza da olanak sağlar. Biz de bu açıdan düşünecek olursak, TTM kullanarak tünelleyen elektronların yüzeyden saçtıkları fotonlar ile çalışma şansı buluyoruz. Eğer tünelleyen elektronlar sayesinde yüzeyden foton çıkışının nedenlerini anlayabilirsek birçok farklı yüzey sistemini TTM ile topografisini görüntülemekle kalmayıp aynı zamanda diğer özelliklerini de inceleme şansı bulacağız.

Young ve arkadaşları tünelleme ekleminden foton saçılmasını öngördüklerinde, henüz TTM icat edilmemişti. Bunun için metal-oksit-metal eklemi üzerinde çalıştılar. TTM'in Binnig ve arkadaşları tarafından icad edilmesi ve ilk başarılı deneyinin yapılması Young'ın öngörüsünü gerçeklendirmeye fırsat tanımıştır.

Gimzewski ve arkadaşları tarafından ilk başarılı deney gerçekleştirilmiştir. Tünelleme ekleminin yanına yerleştirilen bir foto detektör ile tünelleme ekleminden foton çıkışı gözlemlenmiştir. Bu gelişmeler bize daha büyük ufuklar kazandırmış ve tünelleme ekleminden foton saçılımının nedenleri TTM ile daha kolay ve daha çok anlaşılır bir şekilde çalışılmaya başlanmıştır.

İlk başarılı deney de beraberinde birçok araştırma grubunun dikkatini bu konuya çekmeyi başarmıştır. Bu yeni method ile iletken yüzeylerde nano yapıların, yüzey sistemlerinin topografik ve elektronik çalışılmasının yanında optik özelliklerinin de incelenebilmesine olanak sağlanmıştır.

Bizim çalışmamızda da bu çalışmalar örnek alınarak laboratuvarımızda bulunan öğrenci eğitim amaçlı olarak üretilmiş TTM cihazı geliştirilmiş ve gerekli modifikasyonlar yapılarak tünelleme ekleminden foton saçılımı gözlemlenebilir bir deney düzeneği kurmak amaçlanmıştır. İlk sonuçlar da kolay sonuç verebilmesi açısından pürüzlü altın yüzeylerindeki ilk uygulaması gerçekleştirilecektir.

Bu çalışmada ilk etapda hedeflenen, öğrenci eğitim amaçlı olarak üretilmiş basit ama bir o kadar da kullanışlı ve tatmin edici sonuçlar veren TTM'yi modifiye edip bilimsel çalışmalarda kullanılabilir bir hale getirmek. Bunun için ilk etapta tersine mühendislik yapılmış ve öğrenci TTM'si tüm fonksiyonlarıyla nasıl çalıştığı, elektronik ve mekanik tüm mekanizmaları çözümlenmiştir. Çözümlenen bu mekanizma kopyalanarak başka bilimsel amaçlı üretilmiş ve bize daha fazla esneklik sağlayan bir kontrol elektroniği ile öğrenci eğitim amaçlı olan TTM başlığı kontrol edilmiştir.

Yeni kontrol elektroniğinin bize sağladığı avantaj, artık yüzey taranırken aynı anda her bir nokta için foton çıkışı ölçülebilecektir. Bunun yanında çalışmak istediğimiz diğer ölçümler için de bize fazladan kanal sağlamaktadır. Yeni elektronik ile aynı zamanda istediğimiz gibi çıkış aldığımız için başka cihazlar ile yüzey taramasını eş zamanlı olarak gerçekleştirmemize imkân verecektir.

Yeni kontrol elektroniği bize daha sonradan sisteme dâhil edeceğimiz lock-in amplifier ve optik spektrometreyi de kontrol edebilmemize imkân sağlayacaktır. Dolayısıyla yeni kontrol elektroniği ile kontrol etmek bizim için sistemin geliştirilmesi ve daha çok ölçüm yeteneği kazandırılması açısından önem arz etmektedir.

Elimizdeki öğrenci eğitim amaçlı kullanılan TTM elektroniği ile bizim sisteme dâhil ettiğimiz kontrol elektroniği ve verdikleri sinyalleri karşılaştırdığımızda öğrenci eğitim TTM elektroniğinin daha gürültülü sinyal verdiğini görüyoruz. Yeni kontrol elektroniği bizim daha sağlıklı, daha az gürültülü ölçümler almamıza olanak sağlamıştır.

Sistem elektronik olarak hazırlandıktan sonra ikinci aşama optik düzeneğin kurulmasıdır. Optik düzenek TTM başlığından bağımsız bir şekilde hareket ederek tünelleme eklemine odaklanmalıdır. Bu sayede TTM başlığı optik sistemden kaynaklanabilecek titreşimlerden izole bir şekilde çalışması sağlanmıştır.

Optik sistemin genel yapısı şu şekildedir: ilk etapda tünelleme ekleminden saçılan fotonlar küresel olmayan lensin odak noktasına ayarlanır ve tünelleme ekleminden toparlanıp paralelize edilir. Paralelize edilen fotonlar daha sonra ikinci bir lens ya da ayna ile fiberoptik kabloya aktarılır. Fiber optik kablo ile tünelleme ekleminden toparlanan fotonlar detektöre iletilir.

Bu şekilde deney düzeneğimizi kurduktan sonra ölçüm almaya başladık ve sistemimizin oldukça iyi bir şekilde çalıştığını söyleyebiliriz. TTM ile yüzey topografisini çıkartırken aynı zamanda foton saçılım haritasını da çıkartabiliyoruz. Yüzeyden foton saçılımının yüzey topografisi ile arasındaki bağlantıyı çalıştık.

Bu noktada birçok soru ile karşılaşıldı. Yüzeyden, tünelleme ekleminden foton saçılımına neden olan sebeplerin oldukça karmaşık bir yapısı olduğu görüldü. Her bir parametrenin foton saçılımı üzerindeki etkisinin çalışılması için her bir parametrenin çok iyi bir şekilde kontrol edilebiliyor olması gerekir. Ancak elimizdeki imkanlar buna pek müsait değil.

Literatür taraması yaptığımızda görüyoruz ki, yüzey sisteminden foton saçılımını etkileyen birçok faktör var. Kullandığımız TTM iğnesinin sivriliği, malzemesi, açısı, yüzey sisteminin malzemesi, ortam nemi, sıcaklığı, kullanılan altın kaplama ince filmin kalınlığı ve birçok neden yüzeyden foton saçılımını doğrudan etkileyebilmektedir.

Yüzeyden, tünelleme ekleminden foton saçılımına neden olan sebeplerin oldukça karmaşık bir yapısı olduğu görüldü. Her bir parametrenin foton saçılımı üzerindeki etkisinin çalışılması için her bir parametrenin çok iyi bir şekilde kontrol edilebiliyor olması gerekir. Ancak elimizdeki imkânlar buna pek müsait değil.

Bu çalışma süresince alınan sonuçların fiziksel açıklamaları ile çalışmaya pek fırsat bulunamamıştır. Daha çok çıkan sonuçlar üzerinde tartışılabilecek sorular sorulmaya çalışılmıştır zira iki yıl için oldukça uzun ve zor bir projedir.

Bu çalışma için çalışılan iki yıl oldukça verimli geçmiştir ve sıfırdan bu noktaya getirmek oldukça zaman alıcı olmuştur. Proje için birkaç sene daha çalışıldığında bu deney düzeneğinden oldukça verimli sonuçlar alınacağı kanaatindeyim.

Proje için konulması gereken hedefler literatürde de belirtilen foton saçılımını etkileyen faktörlerin kontrol altına alınabilmesi olmalıdır. Literatür taraması yaptığımızda görüyoruz ki, yüzey sisteminden foton saçılımını etkileyen birçok faktör var. Kullandığımız TTM iğnesinin sivriliği, malzemesi, açısı, yüzey sisteminin malzemesi, ortam nemi, sıcaklığı, kullanılan altın kaplama ince filmin kalınlığı ve birçok neden yüzeyden foton saçılımını doğrudan etkileyebilmektedir.

Tezimde ilk etapda TTM ile ilgili ve TTM kullanılarak yapılan spektroskopi ölçümleri ile ilgili teorik ve gerçeklenmiş sistemimiz hakkında bilgi vermeye çalışacağım. Daha sonrasında tünelleme ekleminden uygulanan potansiyele bağlı olarak foton çıkışının gözlemlenmesi ile ilgili teorik ve gerçeklenmiş sistemimiz hakkında bilgi vereceğim.

Elde ettiğimiz sonuçlar, üzerinde tartışmalar ve ileride yapılabilecek önerilerimiz olacaktır. Genel itibariyle aldığımız sonuçlar yüzeyin topografik haritasını çıkartırken bir diğer yandan da foton saçılım haritasını çıkarmak olmuştur.

Almış olduğumuz sonuçlar projenin hedefi doğrultusunda ilerlediğini göstermesi açısından önemlidir ancak bu sonuçlara benzer sonuçlar literatürde bulunmaktadır. Bizim ölçtüğümüz sonuçların literatür ile farkları incelenip literatüre farklı bir açıdan yaklaşılabilir.

1. INTRODUCTION

Understanding the electronic and optical properties in atomic and molecular scale is a great challenge to deal with. Imaging and analyzing materials in this scale had been the main motivation for development of different variety of microscopy and spectroscopy techniques.

As we approach to nanometer scale, the resolution for optical microscope has a limitation known as diffraction limit, which tell us the resolution of the optical microscope can be at most half wavelength of light [1]. The goal of the most of the studies on microscopy and spectroscopy had been to overcome this limits by different techniques. Studies to overcome this limits created varieties of experimental setup, techniques and methods, such as electron [2], x-ray [3], and scanning near field optical microscopy [4], [5], [6]. Confocal microscopy and near-field optical techniques are capable of spatial resolution down to a fraction of a micrometer but these techniques are not enough to understand all physical properties of the materials.

Developments on high resolution microscopy and spectroscopy continue with micro Raman spectroscopy (μRS) [7], surface [8], and tip [9] enhanced Raman spectroscopy (SERS) (TERS) to study vibrational, rotational or other low frequency modes of a material. For example to TERS, a noble metal such as silver coated atomic force microscope (AFM) tip with 20nm diameter and laser spot 300nm in diameter is used to get Raman signal from 55nm in diameter area [9]. In another study, Bruno Pettinger and Jens Steindtner reported 15nm of resolution with tip-enhanced Raman spectroscopy [10]. In their study, they used an STM tip to image a dye molecule and study Raman spectra of the molecule.

In different types of Raman spectroscopy that mentioned above, incident light is used to excite the sample states. Another approach to excite sample materials was exciting the sample with electrons, proposed by R.D. Young in 1972 [11]. In their study, electronic excitations were proposed and secondary electron emission from surface was measured.

In 1986, Gerd Binnig and Heinrich Rohrer reported the first successful tunneling experiment, the Scanning Tunneling Microscope (STM) [12]. STM was leading the surface science studies to more interesting and more challenging areas with tunneling electrons. STM is used to visualize the surface topography of conducting and semiconducting materials in atomic scale with 0.01 nm resolution. In addition to that, STM made many spectroscopic techniques possible for single particles in atomic scale, stimulated by tunneling electrons [13]. After the invention of STM, Gimzewski et al. reported the photon emission from STM stimulated by tunneling electrons [14]. The photon emission from STM at atomic resolution [15] has proven that the resolution limits for this spectroscopy technique could be as high as the imaging limits of STM.

Introduction of photon emission from STM created new opportunities to study the electronic and optical properties of the nanostructures such as nano-wires [16], quantum wells [17] or quantum dots [18] etc. STM is not only used to image nanostructures on metal surface, but also STM makes it possible to investigate the energy spectrum of nanoparticles between metal surface and metal tip [19], [20]. Nano structures, such as quantum dots, show quantum physical properties rather than classical properties. The effects of quantum confinement create differences between the bulk material semiconductors and nanostructured semiconductors in manner of electronic and optical properties [21]. Another important area to study with STM is; it is possible to excite surface plasmons locally between tip and sample. Studies on surface plasmons are very important research area in the field of nano photonics.

The goal of this work is to design, construct and application of experimental setup for observation of photon emission from scanning tunneling microscope and application results on rough Au surface will be presented. Photon emission is due to surface plasmons, located on the surface of a conducting sample. Tunneling electrons induce photon emission by losing their energies during their interaction with surface plasmons. The physical background for photon emission from scanning tunneling microscope, development of experimental setup for photon emission measurements from scanning tunneling microscope, our results, discussions about the results and expected future works will be explained respectively.

2. PHYSICAL BACKGROUND

2.1 Introduction

Scanning probe instruments (SPI) are currently being used in a wide range of applications. One of the early applications of SPI is Scanning Tunneling Microscope (STM). STM has a very complicated theoretical and experimental background for visualizing the surface topography and surface spectroscopy. The main principle of an SPI is using a scanning probe as if a blind person using a stick, to find his way. We are all blind in atomic scale and we need to visualize the surface by a sharp tip by measuring interaction between tip and surface. In principle this is how SPI works.

STM basically measures the tunneling electrons (tunneling current) between an atomically sharp tip and sample surface and then, it visualizes the surface Local Density of States (LDOS) and also topography. Sample can be either conducting or semiconducting material. In an STM, an atomically sharp and perfectly conducting tip is scanning a conducting sample surface, measuring the tunneling current between tip and surface at high resolution, point by point on the surface and keeps tunneling current constant by moving tip vertically. This vertical movement is used to visualize surface topography.

Tip can scan the surface, point by point with a resolution of 0.01 nm with scan piezo ceramics in three dimensions. This capability of the STM let us investigate more interesting topics with high resolution by using tunneling electrons, such as photon emission from surface plasmons stimulated by tunneling electrons.

The physical background in main concepts about quantum tunneling, surface plasmons, and photon emission from the scanning tunneling microscope will be covered briefly in this chapter. More details about the calculations and experimental techniques can be found at the reference articles and books [22], [23], [24], [25].

2.2 Quantum Tunneling

In classical mechanics, an electron with mass m (9.1x10^{-28}g) and energy E moving in a potential $V(z)$ is described by equation **(2.1)**

$$\frac{{p_z}^2}{2m} + V(z) = E \qquad \textbf{(2.1)}$$

In classical mechanics, electron can move either to positive direction or negative direction but, it can just be in the region where $E > V$. **(Figure 2.1)**

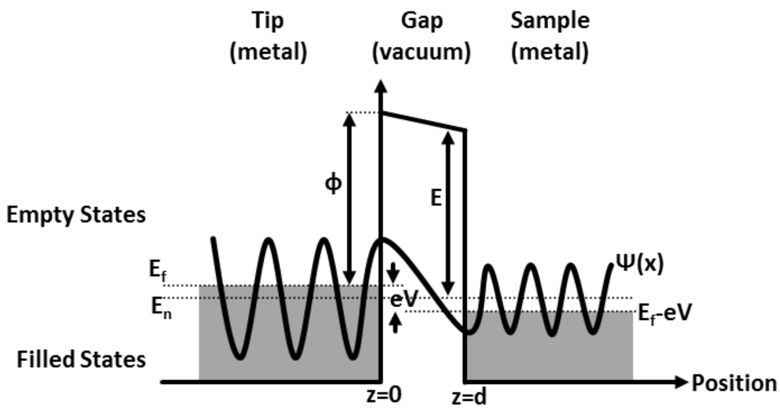

Figure 2.1: Electron tunneling between tip and sample in one dimension.

In quantum mechanics, the same electron is described by wavefunction $\psi(z)$. The Schrödinger equation describes how the quantum state of physical system changes. The Schrödinger equation for this system is **(2.2)**:

$$-\frac{\hbar}{2m}\frac{d^2\psi(z)}{dz^2} + V(z)\psi(z) = E\psi(z) \qquad \textbf{(2.2)}$$

And for the region $E > V$ wavefunction has the solution **(2.3)**:

$$\psi = \psi(0)e^{\pm ikz}\ where\ k = \sqrt{2m(E-V)}/\hbar \qquad \textbf{(2.3)}$$

Different than the classical mechanics, in quantum mechanics, electron can move in the region $E < V$. In this case the Schrödinger equation mentioned above has the solution: **(2.4)**

$$\psi = \psi(0)e^{-\kappa z}\ where = \sqrt{2m(E-V)}/\hbar \text{ , is the decay constant.} \qquad \textbf{(2.4)}$$

To understand the tunneling phenomena, we are looking at the electrons coming from the region where $E > V$ and tunnels to the region where $E < V$. The probability density of observing the electron is $|\psi|^2$ which is equal to $|\psi(0)|^2 e^{-2\kappa z}$. Showing us that electron can be found on the positive side with a decaying but nonzero probability. This information is already a good start for explaining the tunneling phenomena in STM. In an STM metal-vacuum-metal condition is provided by a metal tip-vacuum-metal sample.

The minimum energy required to remove an electron from a bulk to the vacuum level is called work function represented as ϕ. The upper limit of occupied states in a metal at absolute zero temp is called Fermi Level (neglecting the thermal excitations). Fermi energy is equal to work function with minus sign if the vacuum level is taken as the reference point, $E_f = -\phi$. If we assume that the work function of each sample and tip is equal, electron tunneling can occur from sample to tip and also tip to sample but there is no net tunneling current yet. Bias voltage to sample or tip, creates a net tunneling in between tip and sample.

If a bias eV<< ϕ is applied to the tip, a tip state ψ_n, with energy level E_n lying in between E_f and E_f –eV has a probability of tunneling to the sample (Since eV<< ϕ, E_n can be assumed as very close to Fermi level -ϕ.). We already know the wavefunction of the tunneling electron $\psi = \psi(0)e^{-\kappa z}$

The probability of finding electron on the surface of sample is **(2.5)**

$$|\psi(z = d)|^2 = |\psi(0)|^2 e^{-2\kappa d} \textit{ where } \kappa = \sqrt{2m\phi}/\hbar \text{ and } \phi = (E_n - V) \quad \textbf{(2.5)}$$

If we sum over all the tip states between E_f and E_f –eV we can find the relation for tunneling current as follows, **(2.6)**

$$I \propto \sum_{E_n=E_f-eV}^{E_f} |\psi_n(0)|^2 e^{-2\kappa d} \textit{ where } \kappa = \sqrt{2m\phi}/\hbar \text{ and } \phi = (E_n - V) \quad \textbf{(2.6)}$$

We had already mentioned that eV<< ϕ so, E_n can be assumed as very close to Fermi level –ϕ. We can assume that E_n does not change significantly. This relation can also be written in term of the local density of states (LDOS) of the tip at location z and energy E.

LDOS for sample is, **(2.7)**

$$\rho_t(z,E) \equiv \frac{1}{\epsilon}\sum_{E_n=E_f-eV}^{E_f}|\psi_n(z)|^2 \quad \textbf{(2.7)}$$

Relation for tunneling current in terms of LDOS becomes, **(2.8)**

$$I \propto V\rho(0,E_F)e^{-2\kappa d} \quad \textbf{(2.8)}$$

Our system is tip biased system and description for net tunneling current is calculated. There are more details and more explanations about this phenomena about the physical background of STM. More details can be studied from the reference books [22], [23], [24].

2.3 Scanning Tunneling Spectroscopy

STM also makes it possible to locally probe the sample and local electron states with a 0.5nm resolution. The technique is quite simple but not easy. The tip is moved to any position on image and tunneling current is measured with respect to different bias voltages. During STS measurements feedback mechanism is open (not working) and distance between tip and sample is expected to be kept constant. It is very important to isolate the sample from external vibrations to keep the sample-tip gap constant. This technique gives us information about density of states (DOS) of the sample and tip at position of tip.

Density of states is a function of energy, ρ(E). This gives us how dense the states are packed in energy range E+dE. Changing bias voltage changes available energy states for tunneling and tunneling current is a measure of density of states at that energy level. We are making an important assumption during spectroscopy. We are assuming that DOS in the tip is constant, does not change with respect to bias voltage. **(2.9)**

$$I \propto \int_0^{eV} \rho_{sample}(E+E_F)dE \quad \textbf{(2.9)}$$

If we take the derivative with respect to bias voltage it gives us density of states; we end up with **(2.10)**

$$\frac{dI}{dV} \propto \rho_{sample}(E + E_F) \qquad \textbf{(2.10)}$$

Schematic diagram of tunneling spectroscopy and experimental results from ref [26]. dI/dV (differential conductivity) with respect to bias voltage recorded on the (2×1) and c(4×2) domains of a Ge(001) surface systems [26]. **(Figure 2.2)**

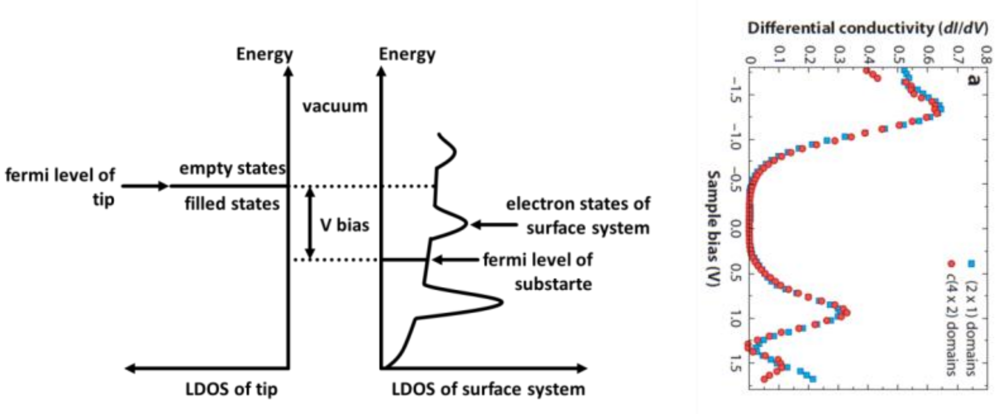

Figure 2.2: Schematic diagram of tunneling spectroscopy and experimental results from ref [26].

More details about STS can be studied on the references [22], [23], [27].

2.4 Surface Plasmons

Surface plasmons are coherent electron oscillations with electromagnetic waves that propagate along the surface of a conducting material mostly metal with negative and complex dielectric constant ϵ (figure 2.4.1 (A)). Actually, these are the light waves trapped on the surface because of their interaction with the free electrons of the conducting material. When free electrons oscillate in resonance with light wave, they trap the light waves collectively. This interaction creates very unique properties named as surface plasmons [25]. The theory behind the existence of surface plasmons is explained on the reference article by Fuzi Yang et.al. [28].

Solving Maxwell's equations in proper boundary conditions show us the interface between a dielectric and a metal can support surface plasmons [28]. The interaction between the surface plasmons and electromagnetic wave changes the momentum. Electromagnetic radiation has momentum $\hbar k_0$ in free space and has a momentum of $\hbar k_{sp}$. Because of binding of surface plasmons to the surface, electromagnetic radiation has greater momentum than free space, $k_{sp} > k_0$ [25]. **(Figure 2.3)**

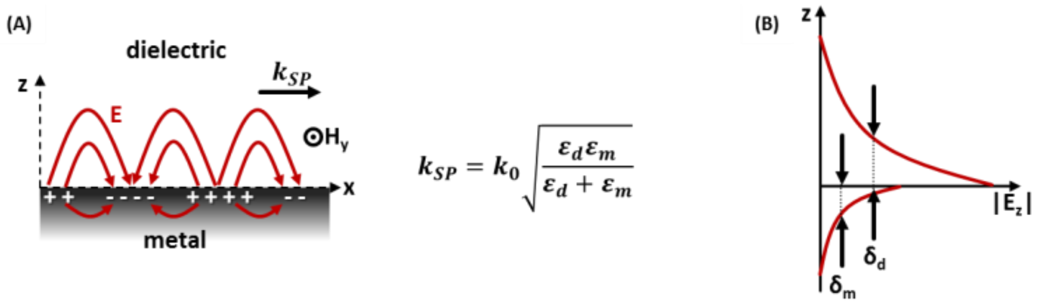

Figure 2.3: Surface plasmons are coherent electron oscillations with electromagnetic waves that propagate along the interface (A) and evanescent field (B).

Another significant result of interaction between surface charges and electromagnetic waves is the field perpendicular to the surface decays exponentially with the distance from the surface. This field is known as evanescent field (figure 2.4.1 (B)). Due to the evanescent field and non-radiative nature of surface plasmons, power cannot propagate away from the surface.

If we send a laser beam at a frequency of surface plasmons resonance, we can create surface plasmons in nanometer range. The surface plasmons have much smaller wavelength than regular photons at the same frequency. The shorter wavelength with surface plasmons brings us the advantage of creating nanoscale optical integrated circuits which are smaller than wavelength of regular photons. Understanding the unusual behaviors of surface plasmons can lead us a new era for ultrafast circuits at nanoscale.

2.5 Photon Emission of Scanning Tunneling Microscope from Surface Plasmons

When two metal surfaces approach to each other very closely, electrons tunnel from one to other surface. Electrons can tunnel from one metal to another elastically or inelastically (figure 2.5.1). We had already mentioned about the elastic electron tunneling in which, electron does not interact with the surface system and does not loses its energy. During inelastic electron tunneling, electrons lose their energy. Tunneling electrons can induce photon emission from surface system. STM systems make it easier and more accessible to study photon emission from surface systems.

Photon emission from tunneling junctions was predicted and observed before STM was invented. Photon emission from tunneling junctions such as Metal-Oxide-Metal structures were observed before STM was invented in 1976 [29] [30]. After the invention of STM, Gimzewski et al. reported the photon emission from STM stimulated by tunneling electrons [14].

In a scanning tunneling microscope, conducting tip and conducting surface forms surface plasmons. Tunneling junction can support localized surface plasmons resonance. The photon emission from tunneling junction occurs when the localized surface plasmons modes get excited by the tunneling electrons and radiative decays [14], [31]. The surface structure or material is an important parameter for excitation and relaxation [32] **(Figure 2.4).**

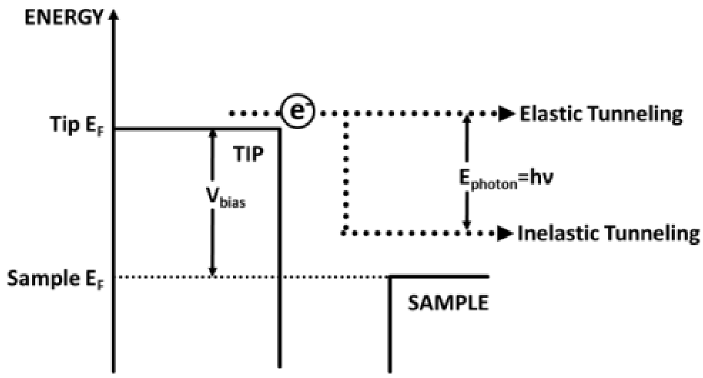

Figure 2.4: Energy diagram of elastic and inelastic electron tunneling.

We didn’t mention about the probability of energy loss in our calculations of electron tunneling but in their calculations, Peter Johansson shows the calculations about the inelastic electron tunneling and photon emission from surface system [33] [34]. I will not get into details of his calculations since it is a very long story and not an easy challenge to understand and explain correctly.

Photon emission is correlated to the surface structure and material, which creates a new method for surface system characterization with an STM system. This technique is like other tip enhanced/optical spectroscopy techniques, but different than them, tunneling electrons are used to excite the surface system instead of incident light beam.

3. DEVELOPEMENT OF A SCANNING TUNNELING MICROSCOPE FROM EDUCATIONAL GRADE TO SCIENTIFIC GRADE

3.1 Introduction

The invention of the STM by G. Binning and H. Rohrer [12] made it possible to image the surface topography of conducting and semiconducting materials' surface with a resolution of 0.01 nm. STM is not only used to image the surface topography but also to study different spectroscopy techniques with tunneling electrons [22]. The main principle of STM is very simple but development of such a stabilized and sensitive system is not an easy challenge. First, the tunneling current is mostly in the scale of nano ampere level or less and it requires very sensitive measurement. Secondly, it is important to scan the surface with the resolution of 0.01 nm which requires moving the tip with a resolution of 0.01 nm. Controlling and measuring this level of current and voltage requires high level instrumentation.

In our laboratory we have a Scanning Tunneling Microscope (STM) system Nanosurf Easy Scan 2™ for student educational purpose, working in ambient conditions. The first step of my studies was to modify this student educational purpose STM system and upgrade the system into a professional and scientific purpose, high-level stm system **(Figure 3.1)**.

Figure 3.1: Nanosurf Easy Scan 2™ STM System for student educational purpose consists of an STM head (A) and an STM control electronics (B).

Chapter 3 will mainly focus on the working principle and instrumentation for a scientific purpose STM. More details than I mentioned here can be found at reference text books [22], [35]. In this chapter, you can find some general information about STM, main working principle of our student educational purpose STM and upgrading our student educational purpose STM into scientific purpose STM, respectively.

3.2 Scanning Tunneling Microscope

When two metal surfaces approach very close to each other, electron tunneling occurs between these two surfaces. Electrons tunnel from one to other in both directions and net tunneling current can be considered as zero. When we apply a bias voltage to one of these surfaces, then we have a net tunneling current in one direction. If one of the metal surfaces is etched or processed to make it atomically sharp, electron tunneling occurs between the top of this sharp surface and other flat surface. Atomically sharp surface means there should be ideally, just one or few atoms at the top of the surface. This sharp surface will be called as tip and will be used to scan and visualize a topographic image of the other surface with high resolution.

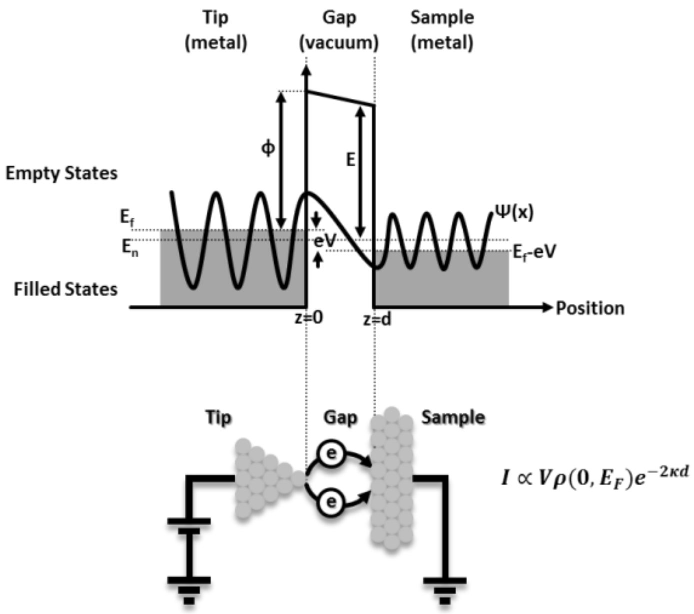

Figure 3.2: Tunneling electrons between two surfaces and its application in STM.

As it is shown in chapter 2, net tunneling current depends on both number of states between E_f and E_f-eV and the distance between the surface and the tip. If we change the bias voltage and keep the distance constant between tip and sample, the number of states between E_f and E_f-eV will change and tunneling current will change. This is also valid for the distance. If we change the distance between tip and surface, tunneling current will change.

There are two different way of imaging surface with an STM: constant current mode and constant height mode. The key feature for constant current mode is feedback electronics, which keeps the tunneling current constant by controlling the piezo on z axis. The z-piezo is responsible for vertical distance between tip and sample surface. Tunneling current changes, if the distance "d" between tip and sample changes.

$$\text{Tunneling Current: } I \propto V\,\rho(z=0, E_F)\,e^{-2\kappa d} \qquad \textbf{(3.1)}$$

The feedback mechanism of an STM always compares the set value of the tunneling current given by the user, with the measured, real time value of the tunneling current. When measured tunneling current is not equal to set value, the difference between the measured value and the set value is amplified and applied to z-piezo. This applied voltage retracts or approaches the tip and sets the distance between tip and surface in such a position that real tunneling current value gets equal to set value. V_z is also measured by the control electronics and it is recorded as the height of the point coordinates.

The surface is scanned by x-piezo and y-piezo which moves the tip on the x-axis and y-axis respectively. Tip scans the surface point by point at a resolution that user sets. At each point, the coordinates of point and height of the tip is recorded. V_x and V_y is recorded as x and y coordinates respectively. When the current is equal to set value, V_z is recorded also as the height of that point. V_x,V_y and V_z values are plotted on 3D graph. This 3D graph can be considered as the map of the surface topography image **(Figure 3.3)**. The second method for imaging the sample surface is constant height mode. In this mode tip is kept at a constant height and surface topography is obtained with respect to the change in tunneling current. This is not an efficient way, since surface has unpredictable topography.

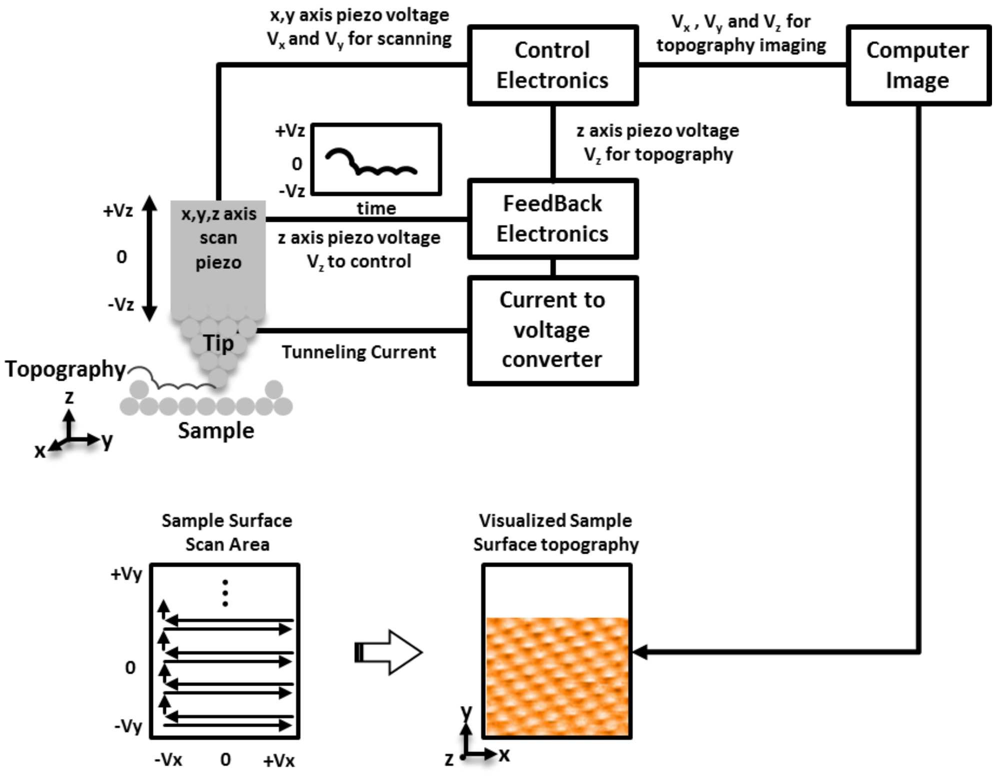

Figure 3.3: Operation principle STM scanning HOPG sample surface.

Keeping the height of tip constant can cause tip crash or tip sample spacing can exceed the tunneling range and we can lose the signal. Tip crash means, tip can hit the surface and lose its sharpness **(Figure 3.4)**. Because of these reasons, constant height mode is not preferable.

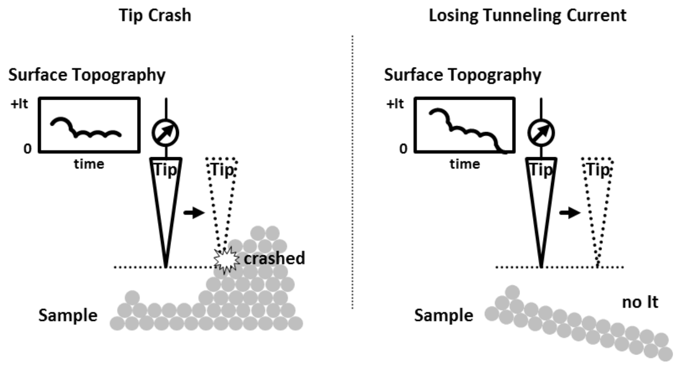

Figure 3.4: Possible errors on STM, scanning surface at a constant height mode.

The resolution of the image also depends on sharpness of the tip. If the tip is sharper, electron tunneling will concentrate on a very small point. (Δx will be smaller on figure 3.2.4) If tunneling current occurs on a very small point, tunneling current will change when there is very small morphological changes on the surface, so imaging will have higher resolution. If tip is not sharp enough, tunneling will be from many points of tip and surface will be imaged in lower resolution. If we consider the top of sharp surface as a sphere, when its radius is 10nm, electron tunneling, so current will concentrate on a very small area with $\Delta x \approx 1.4$nm **(Figure 3.5)**. We can image surface topography in high resolution.

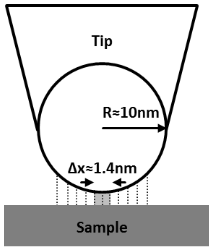

Figure 3.5: Estimated tip shape at tunneling junction for high resolution imaging.

3.3 Upgrading Scanning Tunneling Microscope

Nanosurf Easy Scan 2™ STM is very well functioned for educational purpose **(Figure 3.6)** but not enough for us to do scientific research. It is already mentioned that; during surface scan, V_z is measured and saved for imaging at each scan point. There are more parameters necessary to be measured, saved and plotted but control electronics of this system is offering very limited options. We can only plot and visualize V_z and I_{tunnel}. We need to measure photon emission or dI/dV simultaneously with tunneling current and Vz to work on the dependencies of these parameters to each other.

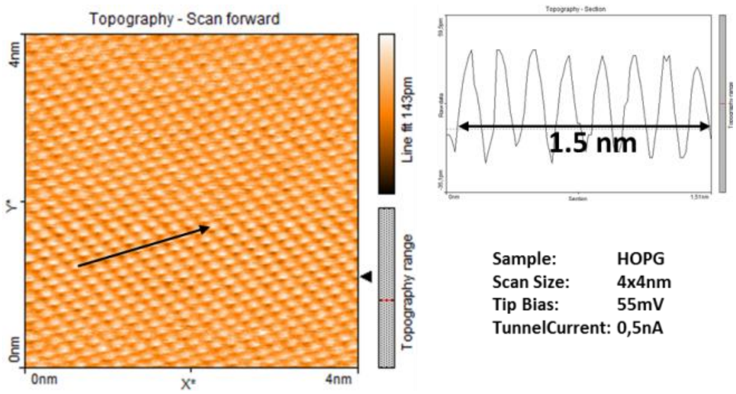

Figure 3.6: Image of HOPG surface scanned with Nanosurf Easy Scan 2™.

This STM head has convenient design that let us get almost scientific grade measurements and image the surface. It also has a good design for sample and tip positions, which makes this STM head suitable to setup an optical system on top of it and measure the photon emission from the tunneling junction. Unfortunately, this system and control electronics has very narrow limits to study on it. It is mandatory to have extra channels for the measuring photon emission, dI/dV and d^2I/dV^2 etc. simultaneously with tunneling current and topography. Another con about the control electronics of this educational purpose student STM is the electronics is unstable and very noisy for a scientific measurements. It is a must for a scientific grade measurement to be stable and noiseless. It was decided to use the STM head of this system but the control electronics will be replaced with more scientific grade STM control electronics.

We decided to use the STM head of our Nanosurf Easy Scan 2™ system as STM head of our Photon Emission of Scanning Tunneling Microscope (PE-STM) system and Nanomagnetics Instruments™ STM control electronics for control electronics of the PE-STM system. The most important reason to choose Nanomagnetics Instruments™ is; it is so easy to get support from the company for our unique setup in software and hardware manner. Neither Nanosurf nor Nanomagnetics has a ready to use setup like we are working on. Another reason for using the Nanomagnetics Instruments™ control electronics is, it can also be used to control our Ultra High Vacuum (UHV) STM system. For future works it is planned to use the optical system and our experiences to develop the same system into an UHV STM and study on the photon emission of STM on UHV conditions.

The basic operational principle of STM head is already well-known and explained in chapter 3.2. However it is already known information, Nanosurf Easy Scan 2™ has its own unique mechanism and the company is not sharing this kind of commercial information. The first step to take for this study was reverse engineering. Operational mechanism of the system is figured out.

3.3.1 Communication between STM head and control electronics

We started from cracking communication between the control electronics and STM head. Communication is done by 25 wires which are connected with 25 pin connections but all pins and wires and their functions were unknown. We made the spy box which was connected between Nanosurf Easy Scan 2™ the STM head and control electronics **(Figure 3.7)**.

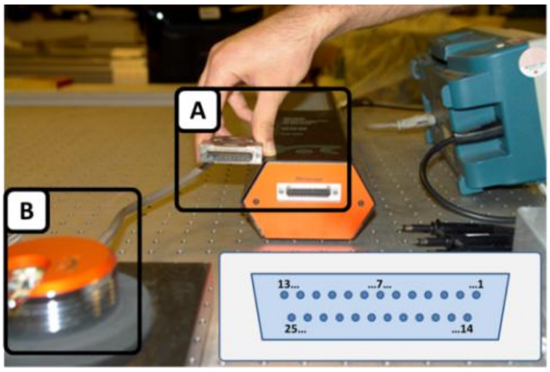

Figure 3.7: Nanosurf Easy Scan 2™ STM head (B), and 25pin connectionor (A).

Each pin has an extra parallel output, connecting each pin to a BNC connector. These extra BNC connectors were spying on the signal without any loss or modification. We measure the signal applied from each pin during operation**(Figure 3.8)**. The basic functions to run STM head are clear and well known. Controlling coarse approach piezos and scan piezos in three dimensions, measuring tunneling current, and applying bias voltage are basic functions controlled by STM electronics on STM head. Spying on each pin with an oscilloscope, we figured out the function of each pin one by one regarding on the basic principle of STM.

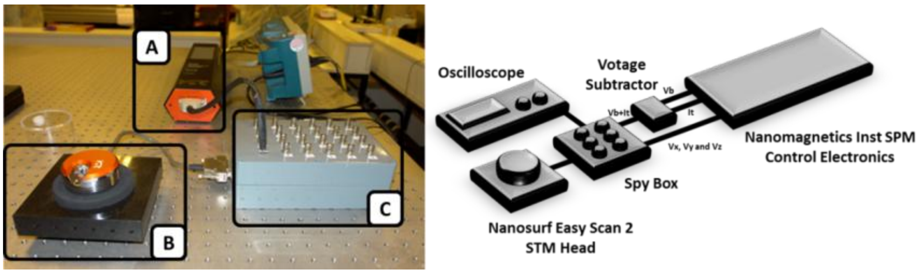

Figure 3.8: Schematic: spy box (C), STM head (B), and control electronics (A).

The tunneling current between the sample and tip is in the range of 0.1nA to 50nA. Measuring such low current amplitude is not easy for electronics since the noise due to the external electromagnetic waves is more than 1 μA. A current amplifier right after the tunneling junction is essential for this kind of a measurement. The tunneling current is converted into voltage by Operational Amplifier (OpAmp) inside the stm head right after the tip. Tunneling current is applied to inverting input of OpAmp. There is a 10^8 Ohm FeedBack Resistor (R_{FB}). R_{FB} sets the amplification coefficient. 1nA is amplified into 100mV in our STM head **(Figure 3.9)**. The formula for voltage output of OpAmp is, $V_{OUT} = -I_{IN} \times R_{FB}$. This voltage output is connected to the stm control electronics by pin no2.

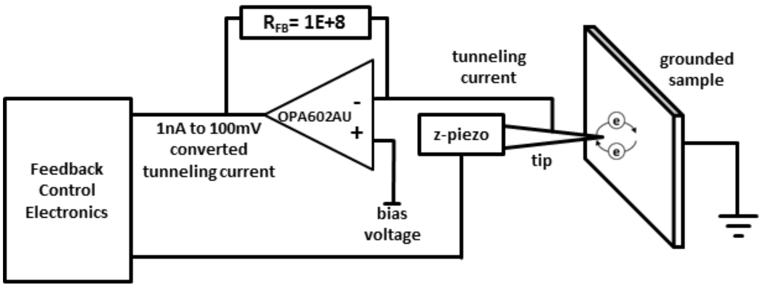

Figure 3.9: Operation schematic of tunneling current measurement.

There are two ways of applying a bias voltage to get a net tunneling current. Bias voltage can be applied either to tip or to sample. Our system is a tip biased STM and sample grounded. There is a little trick in the system. Bias voltage is not applied to the tip directly. Bias voltage is applied to non-inverting input (V+) of the OpAmp. This method sets an offset voltage to inverting, non-inverting input and output of OpAmp in amount of bias voltage. Since tip is connected to inverting input of OpAmp, tip has bias voltage. The bias voltage is applied by pin no4.

It was mentioned before that the Nanosurf system is a student educational purpose STM, so to reduce student based mistakes that could be done by students, there is a stm head check signal sent with pin no5. When the electronics is turned on, pin no5 applies 15V and checks if the STM head is connected properly. This pin is not necessary for us and we are not going to use it for our system.

Tunneling between tip and sample occurs in the range of less than one nanometer. It is not possible to arrange the spacing between sample surface and tip, by hand. Vibrations due to pulse on our hand or floor vibrations is more than 0.1 mm. When tip starts approaching to surface it should be isolated from user and floor vibrations. STM head has its unique mechanism to approach surface to tip. This coarse approach mechanism let us arrange the spacing between sample surface and tip, less than 500nm. Sample approaches with sample holder through tip with two coarse approach piezo ceramics, controlled by pin no 6 and 8. Tip keeps its position constant and stable. The surface topography is imaged by recording z piezo voltage corresponding to each coordinates and three dimensional images are obtained. Three scan piezo ceramics are moving tip in three dimensions. Scan piezo ceramics in x,y and z axis are controlled by pin no 10, 12, and 13 respectively. The connections and pin map between stm head and control electronics is shown in table. The connections in the STM head circuit is shown in **Figure 3.10, Table 3.1**.

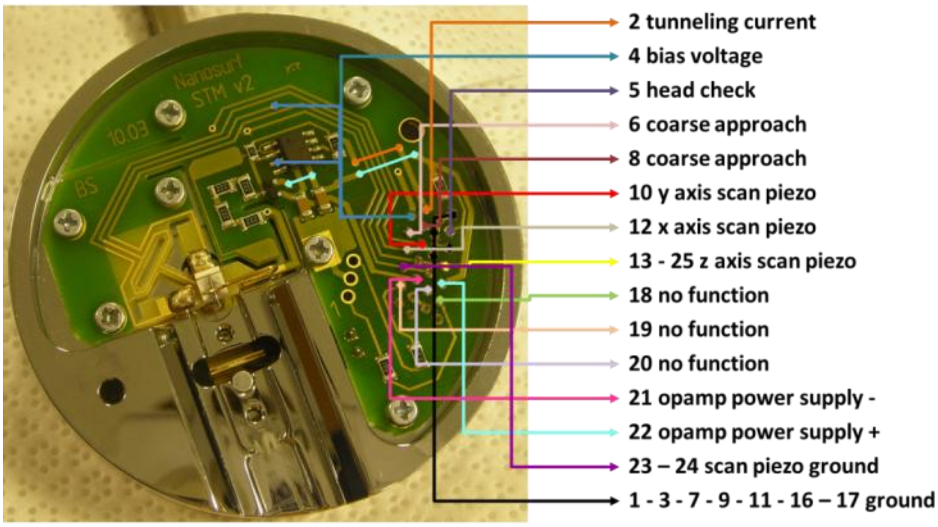

Figure 3.10: STM head, top view of circuit board and functions of each pin.

Table 3.1: Functions of each pin.

Pin Number	Function
1	Ground
2	Current to Voltage converted Tunneling Current
3	Ground
4	Tip Bias
5	Checks if the STM head is connected to the electronics.
6	Coarse Approach Piezo Control No.1
7	Ground
8	Coarse Approach Piezo Control No.2
9	Ground
10	Scan Piezo in Y-Axis (±10 V)
11	Ground
12	Scan Piezo in X-Axis (±10 V)
13	Scan Piezo in Z-Axis (±10 V)
14	Not Connected
15	Not Connected
16	Ground
17	Ground
18	No Function
19	No Function
20	No Function
21	STM head OpAmp (OPA602AU) power supply -15V
22	STM head OpAmp (OPA602AU) power supply +15V
23	Offset Voltage for Scan Piezo in X and Y Axis
24	Offset Voltage for Scan Piezo in X and Y Axis
25	Scan Piezo in Z-Axis (±10 V)

3.3.2 Sample approaching

Approach mechanism design is one of the key features to get clear, stable, and low noise images from the surface with STM. It is important because it sets how tip and sample will stay after tunneling occurs. If tip and sample stay more stable, image will be more clear. Approach can be done either by moving tip or moving sample depending on design of STM. In our system sample is moving to approach tip.

To start with, let me explain the main structure of the approach mechanism. Sample holder moves through the tip and approaches very slowly. Sample holder has an easy and efficient design to work with. We are pasting our sample on sample holder using a good conductor such as silver paste. Conducting paste used to be sure that there is an electrical contact between sample holder and sample surface to ground well the sample. A perfect electrical contact is essential since the sample must be grounded perfectly. Sample holder, with sample on it, is placed on to sample holder holder cylinder. There is a small but strong magnet to hold sample holder on cylindrical sample holder holder **(Figure 3.11)**. This makes it easy to change the sample holder without conducting paste.

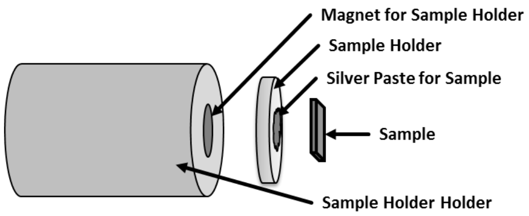

Figure 3.11: Sample and Sample Holder.

Sample holder holder is the main part responsible for moving and approaching the sample to tip. It has to be fat free, perfectly cleaned, and conductive since it is in contact with ground. It is also essential to move holder with coarse approach piezo **(Figure 3.12).**

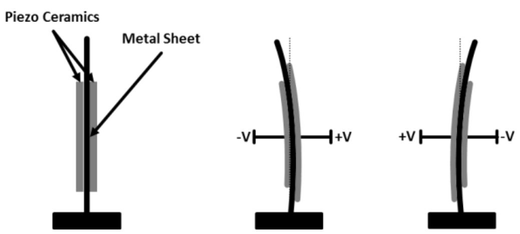

Figure 3.12: Coarse Approach Piezo.

When the system is at rest and there is no tunneling current, both coarse approach piezo and z axis piezo stay in position “0”. When the user, so the software send approach command to the control electronics, first, z-piezo takes position “I” very fast. This position of the z-piezo keeps the tip away from the sample as far as z-piezo can. There will be enough space for sample to approach tip. This space is more than each step of the sample, so when the sample approaches to the tip, it will not crash. Then, the coarse approach piezo take position “II” slowly in about 5 ms, so the sample holder slides forward about 100nm with the coarse approach piezo. Later, the coarse approach piezo takes position “III” very fast in less than 1ms, so that the sample holder does not slide backwards with the coarse approach piezo. After that, the coarse approach piezo takes position “0” slowly again in 5 ms, so that, the sample holder slides forward about 100nm with the coarse approach piezo again **(Figure 3.13)**.

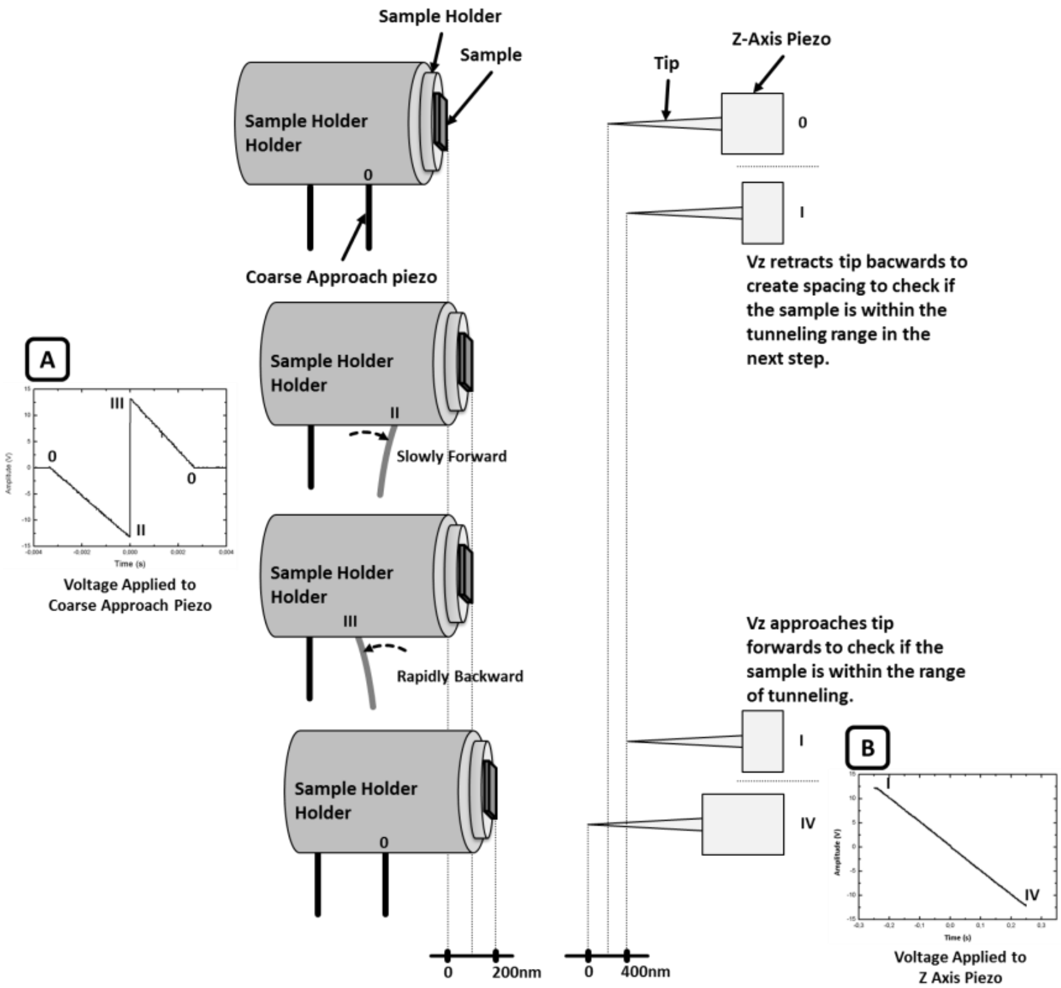

Figure 3.13: The basic operation of approaching sample to the tip.

After all, the sample is moved forward with coarse approach piezo in 200 nm. Finally the z-piezo gets the position “IV” from position “I” very slowly about 500 ms. While z-piezo is moving from position “I” to “IV” feedback mechanism is closed and checks if the tip is in the distance of tunneling, by measuring the tunneling current at each step. The step size can be down to 1 pm. If the separation between the tip and sample is not close enough for tunneling, all this process is repeated until the tunneling occurs. The sample tip spacing is measured between 0.1 nm to 0.4 nm. [22], [36].

3.3.3 Surface imaging

In stm instrumentation, scan piezo ceramics are the key point of imaging the surface with highest resolution. Piezo ceramic scanners can achieve fine tip movement in three dimensions in a limited range but highest resolution. Piezo ceramics change their shape when an electric field is applied. The other way is also valid. If the shape of piezo ceramics is changed, an electric field inside piezo ceramics occurs **(Figure 3.14)**.

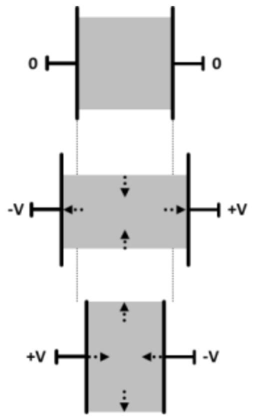

Figure 3.14: Piezo Ceramics and their response to electric field.

Piezo ceramics surfaces are coated with a conducting metal. To create an electric field inside piezo ceramics, voltage is applied to metal coated surface of piezo ceramics. It is possible to change the shape of piezo ceramics down to 0.01 nm. depending on sensitivity of control electronics. In our system, tip is attached to the piezo ceramics. When the shape of the ceramics change, tip position changes. Mostly control electronics can achieve 0.1nm resolution in x and y axis but 0.01 nm resolution in z axis. This surprising result in z-axis is due to working principle of the feedback electronics. In our system to extend shape of piezo ceramics 204.9 nm, 10V must be applied and to shrink the shape of piezo ceramics 204.9 nm, -10V must be applied. Resolution of our piezo ceramics is ~20,4nm/V. Generally scan piezo ceramics work in the range of high voltage but as we mentioned before this is a student educational purpose STM and high voltage is high risky and dangerous for this purpose. This property of our STM has pros and cons. It is mentioned that it is not risky but, this system has 10 times less tolerance for electronic noises **(Figure 3.15)**.

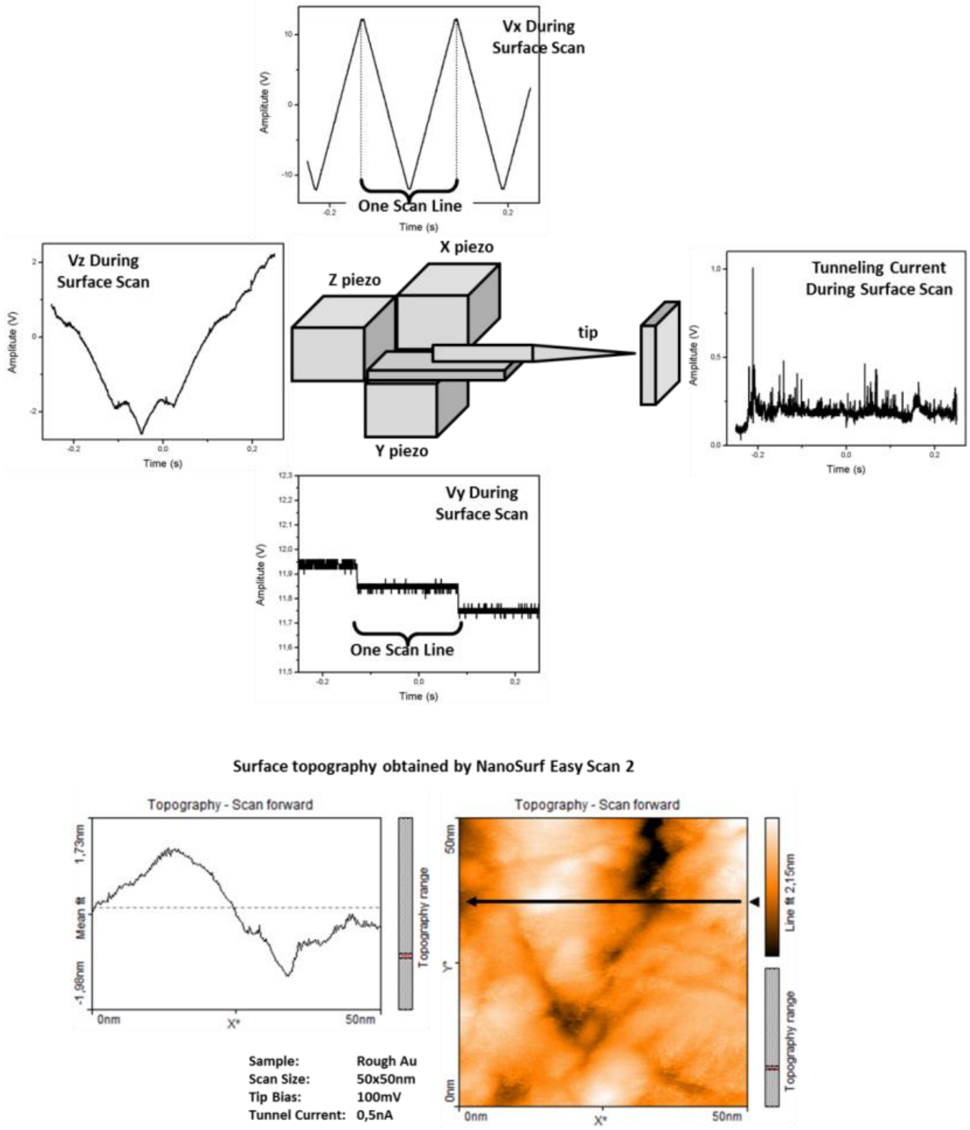

Figure 3.15: Voltage applied to scan piezo ceramics in three dimensions to scan sample surface and Rough Au surface obtained by Nanosurf Easy Scan 2™.

One of the most important parts of the STM for high resolution is tip. It is a great challenge to prepare an atomically sharp tip. It was mentioned before as the sharpness of the tip affects the resolution and morphological image obtained from the surface. One of the most challenging parts of working in ambient conditions is tip crashes. We had investigated the change in the image when the tip crashes to surface or any other molecules or structures from surface sticks on tip. It is almost impossible to know exactly what happened to the tip but we had can see its effects on the image during scan (**Figure 3.16)**.

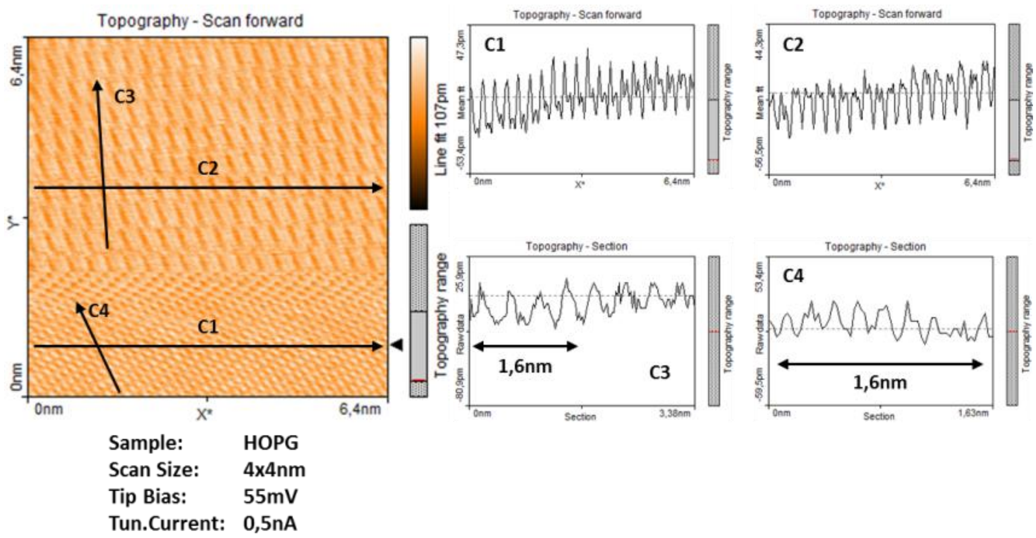

Figure 3.16: Changes on the image during surface scan due to tip crash or when any surface atom sticks to tip and changes the shape of top of tip.

3.3.4 Vibrational isolation

Isolation of the system from environmental vibrations is essential when your research is in atomic scale. The vibrations from the building or acoustic vibrations affect the distance between the tip and surface so tunneling current is affected. For instance, to have a resolution of 10 pm in vertical range, tip sample spacing is required at 1 pm scale [22]. This spacing is 10^5 times less than the floor vibrations which are assumed to be about 1 micrometer. It is impossible to take a perfect image of the sample surface or do spectroscopic measurement of surface system without vibration isolation. Even the traffic on the road 200mt away from our laboratory can affect the measurements badly make them very noisy. An optical table with active supports isolates our system from external vibrations.

3.3.5 Integration of SPM control electronics to STM head

After reverse engineering the working principle of Nanosurf Easy Scan 2™, Nanomagnetics SPM control electronics was modified for the STM head. Calibrating and Testing an STM system can be done by imaging well known surface structure with well-known parameters such as Highly Oriented Pyrolytic Graphite (HOPG) surface. HOPG became a common calibration surface after the studies on HOPG with STM [37], [38]. HOPG has a layered structure and at every layer carbon atoms form hexagonal lattice with cell coefficients: a: 0.2456nm, c: 0.6711nm **(Figure 3.17)**.

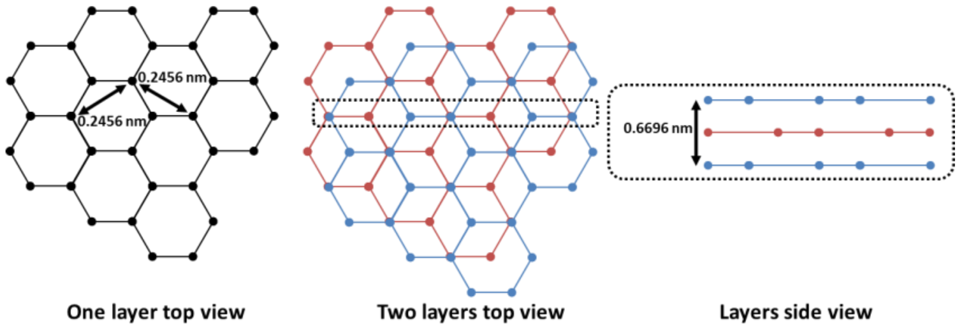

Figure 3.17: Highly Oriented Pyrolytic Graphite (HOPG) crystal structure.

Each monolayer has height of 0.35nm approximately. We had scanned an HOPG surface and measured the height of the layers. We had measured the height of a layer as 1.05nm which is exactly 3 monolayers ($3 \times 0.35nm = 1.05nm$). **(Figure 3.18)**

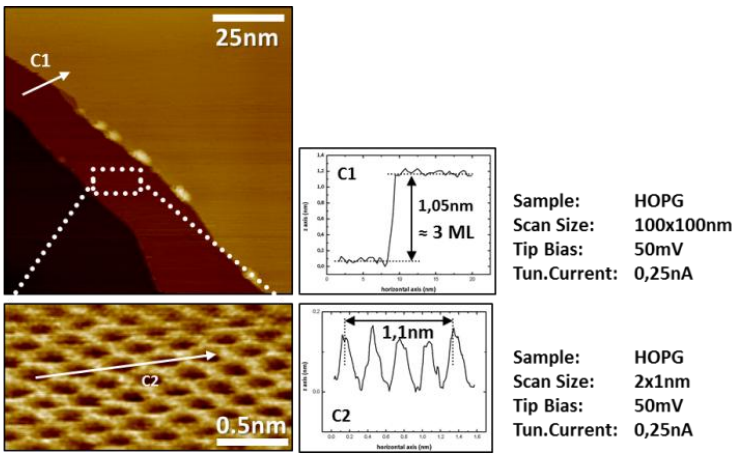

Figure 3.18: The STM image of HOPG imaged with upgraded system

It was mentioned before as there was a little trick for applying bias voltage. Offset voltage was set on non-inverting input and this offset was applying bias voltage to the tip. This simple trick for applying bias voltage also caused another problem for control electronics. Tunneling current was converted into voltage with a gain factor of 1nA to 100mV but tunneling current was measured with an offset voltage in amount of bias voltage **(Figure 3.19)**.

Figure 3.19: Bias voltage subtractor box and circuit schematic

For example, if we set bias voltage to 100mV and tunneling current to 0.5nA, we should measure tunneling current as 50mV but we are measuring 50mV+100mV. This 100mV comes from the bias voltage. For real time measurements bias voltage subtracting circuit was designed (figure 3.3.5.3). and added to the system between STM head and control electronics (figure 3.3.5.4). Real time measurement of tunneling current is essential for spectroscopic studies such as I/V spectroscopy and dI/dV spectroscopy **(Figure 3.20)**.

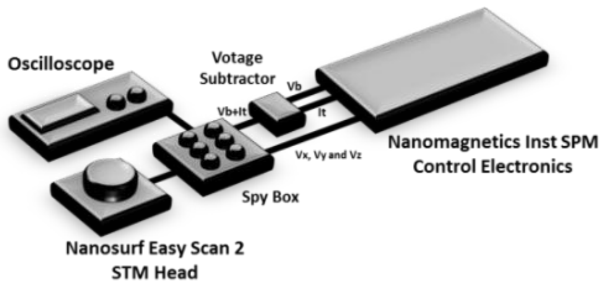

Figure 3.20: Schematic representation of STM system with bias voltage subtractor

It was already mentioned that our scan piezo ceramics are not working with high voltage and due to this property; we don't have noise tolerance very much. Voltage to piezo displacement rate is ~20.4 nm/V, this means if we apply 1 V to scan piezo, tip displacement is 20.4 nm. Scan piezo output from Nanomagnetics control electronics is measured and there is approximately 50mV peak to peak noise. This means 0.102 nm noise on piezo and tip position. This is not perfect but a convenient result for our system.

Noise in our system is because of not only the control electronics, but also noisy ground. If grounding on the system is not very well this will directly affect the imaging. We had investigated this problem by mistake. The circuit board of STM head has two sides. We had investigated the top side of the STM head but we didn't remove this board and investigate the bottom side not to take any risk of breaking the circuit. Since there is no signal on the ground side of the piezo ceramics, we didn't measure any signals on pin no 23 and 24 and didn't realize that these pins were scan piezo ceramics ground **(Figure 3.21)**.

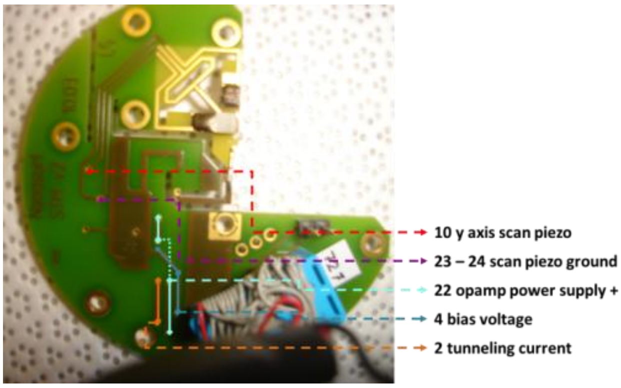

Figure 3.21: Bottom side of the STM head circuit board

Piezo ceramics contacts acts like a capacitor. When there is a potential difference between two sides it forms an electric field inside piezo ceramics and this electric field make piezo ceramics change its shape and tip position. If ground side is not always zero, controlling potential difference between piezo ceramics becomes hard. We had examined this effect in some of our images but later we had grounded the piezo ceramics and problem solved **(Figure 3.22)**.

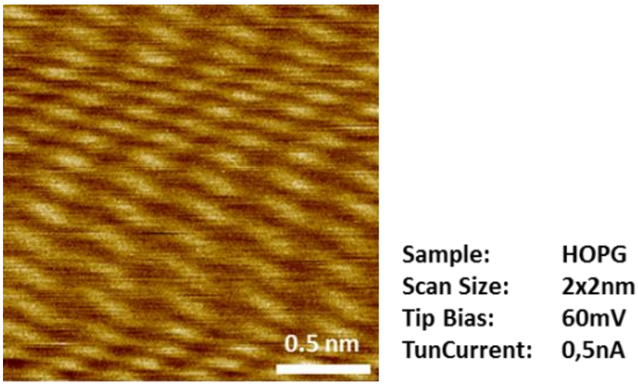

Figure 3.22: HOPG surface imaged with our un-grounded system.

Another noise source was spy box that we developed. It was in a plastic box and was not shielded. We made another version for spy box which is inside an aluminum shielded box. We also reduced the number of connections to reduce the noise. On this box we have It, Vb, Vx, Vy, Vz, approach piezo control pins and power supply. After all this challenges we can control our STM head and get surface images with known parameters and proof that our system is working properly **(Figure 3.23)**.

There are other images below for calibration. We are ready to setup our photon collection setup to measure the photon emission from tunneling junction.

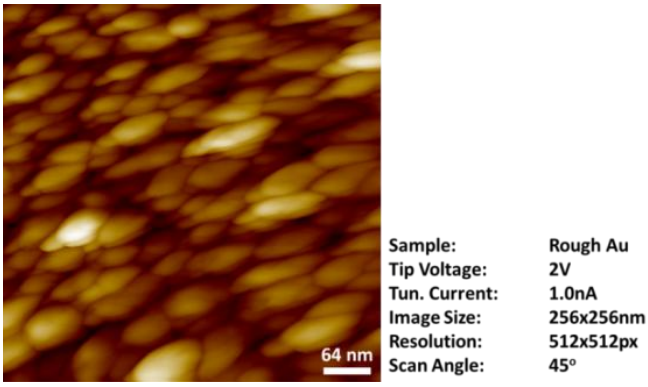

Figure 3.23: Rough Au surface imaged with our upgraded system.

3.3.6 Scanning tunneling spectroscopy, I/V and dI/dV measurement

Inelastic electron tunneling can be observed on dI/dV and d^2I/dV^2. The effect of inelastic tunneling in I/V spectrum is very weak but Persson and Baratoff expected to observe this effect by taking the second derivative of the tunneling current with respect to bias voltage [39], [40]. The experimental results of first sample Acetylene on Cu (001) is shown [41]. We had developed our system considering this effect **(Figure 3.24)**.

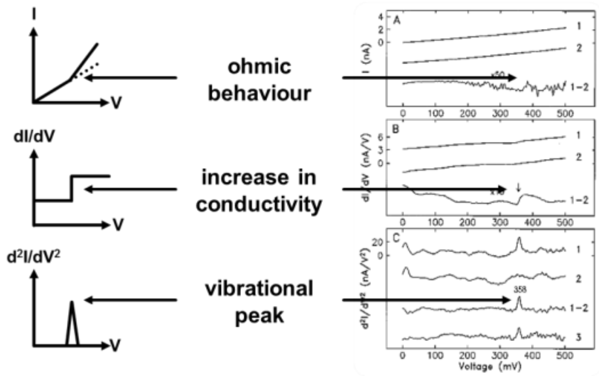

Figure 3.24: Effects of photon emission on I/V, dI/dV and d^2I/dV^2 spectroscopy.

In theory, it is possible to take the first derivative of I/V curve and calculate dI/dV curve but in real life experiment it is not possible because of noises on tunneling current due to external electromagnetic waves or mechanical vibrations **(Figure 3.25)**, and **(Figure 3.26)**.

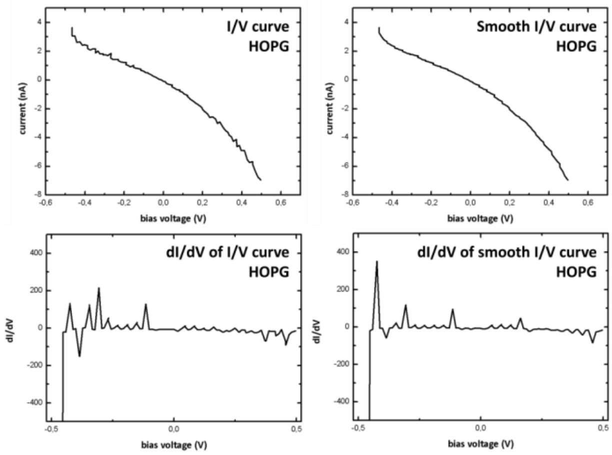

Figure 3.25: I/V and calculated dI/dV curve on HOPG surface

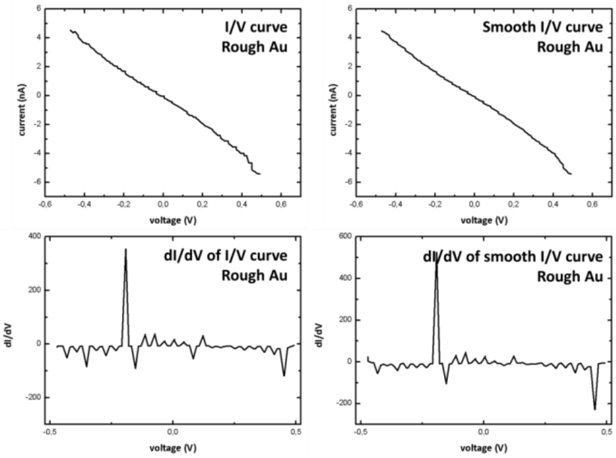

Figure 3.26: I/V and calculated dI/dV curve on Rough Au surface

As it is shown on both two graphs above, calculating I/V curve does not give us meaningful information. We also tried to smooth the I/V curve to reduce the external noise and take derivative but this method also did not work. We need to measure dI/dV simultaneously with I/V curve during experiment. This method is quite challenging to understand and realize the setup **(Figure 3.27)**.

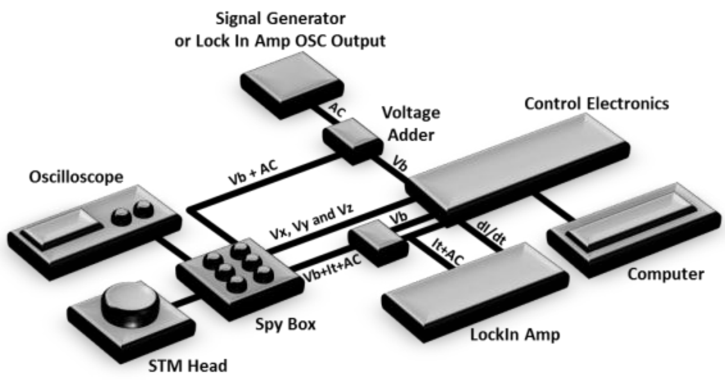

Figure 3.27: Schematic representation of our STM system capable of STS

We will measure dI/dV by using a Lock In Amplifier. Ideally, we are coupling a perfect sinusoidal signal with small amplitude and high frequency to bias voltage. This signal can be observed on tunneling current at the same frequency. Measured tunneling current with sinusoidal wave is tunneling current without external noises. If we can extract the sine wave from measured output and subtract the sine wave, this will give us tunneling current without noises. Lock-In Amplifier does this operation. Lock In Amplifier theory tell us that if output signal of experiment is perfectly linear coupled to sinusoidal driving signal, the output of lock in amplifier will be first derivative of driven signal. This sinusoidal signal frequency should be more than the feedback mechanism can response and stm electronics will not recognize the sine wave in tunneling current **(Figure 3.28)**.

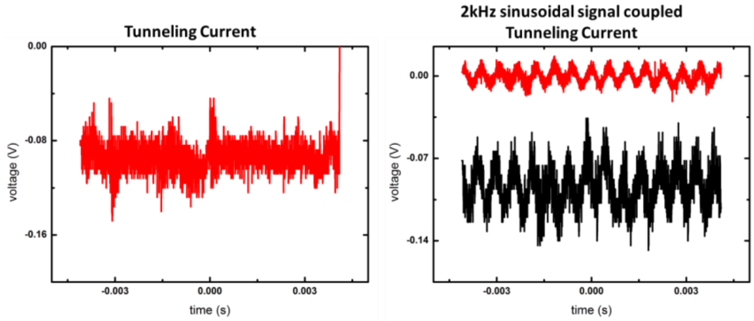

Figure 3.28: Tunneling Current (A) and 2 kHz sinusoidal signal (red) coupled Tunneling Current (black) (B)

We will measure the output of lock in amplifier output for dI/dV spectroscopy. We made two different voltage adder circuits with two different methods to add bias voltage and sinusoidal signal **(Figure 3.29)**.

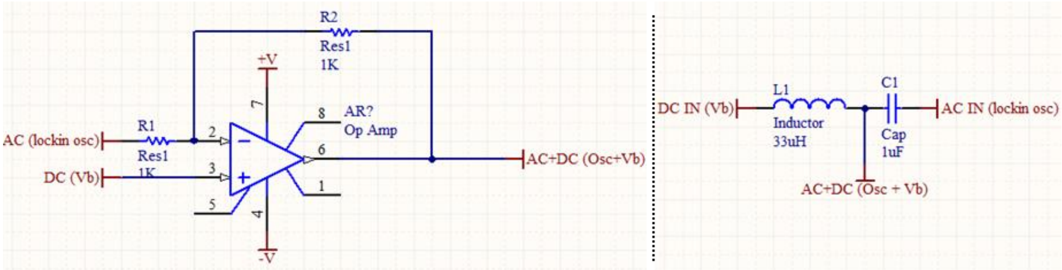

Figure 3.29: Voltage adder circuit with two different methods.

We had tested our system if it works when we add an AC signal to bias voltage. We had scanned the same surface with two different AC signal sources. One is signal generator and the other is lock in amplifier. The surface topography is obtained as the same with sinusoidal signal added to bias voltage DC source is bias voltage and AC source is signal generator and lock in amplifier. We don't see any effects of adding AC signal on bias voltage, on image. **(Figure 3.30)**.

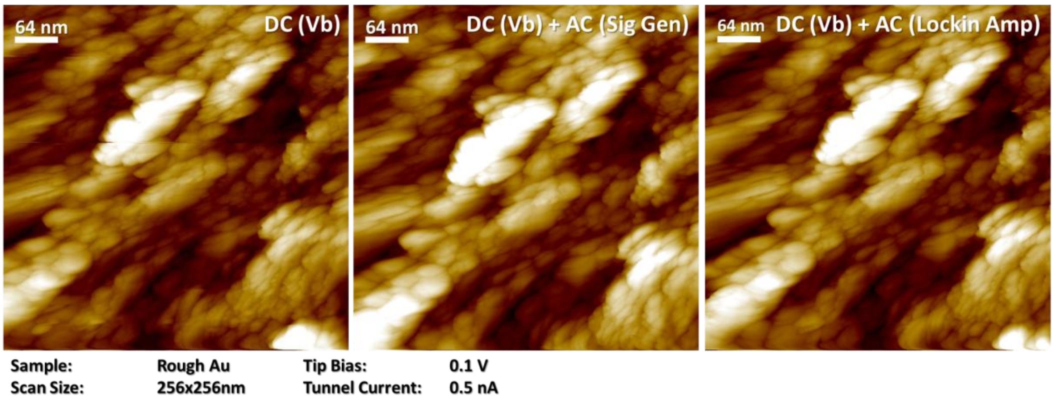

Figure 3.30: Rough Au sample is scanned with DC only and DC+AC.

I could not make any dI/dV measurement since we did not have a working Lock In Amplifiers when I was in the project but I know that this system works properly. Tht group received the Lock-In amplifiers at the week I left the group and they were able to get the first and second derivative of I/V measurements.

4. PHOTON EMISSION FROM SCANNING TUNNELING MICROSCOPE

4.1 Introduction

Photon emission from Scanning Tunneling Microscope (STM) was proposed by young in 1972 [11] before the invention of STM. After the invention of the STM by Gerd Binnig and Heinrich Rohrer [12] the first successful experiment reported by Gimzewski et al. in 1988 [14]. They placed a photodetector near the tunneling junction and measured isochromatic photon emission from tantalum and Si (111) 7x7 surface system. After this experiment, experimental studies on photon emission from surface systems using tunneling electrons with scanning tunneling microscope became realizable and attracted the attention of many researchers. Many experiments on photon emission from scanning tunneling microscope have been investigated since then [42], [43], [44], [45], [46] etc.

The first successful experiment was done by placing a photomultiplier tube close to tunneling junction [14]. New techniques to collect and measure the emitted photons were developed and more optical components such as mirror [47], lens and fibers [42] were used to collect and investigate the photon emission from tunneling junction (**Figure 4.1)**.

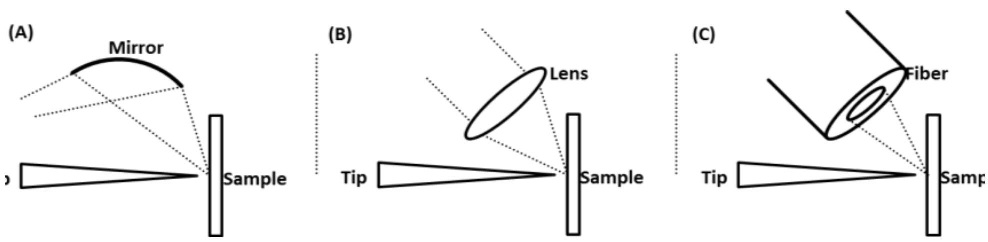

Figure 4.1: Collecting photons with Mirror (A), Lens (B) and Fiber (C)

All these different techniques have their own challenges but one aim: to collect emitted photons at maximum intensity. Photons are emitted from a single point photon source; tunneling junction. Photon emission forms a hemisphere above the sample surface. The intensity of the emitted photons is very low. To collect emitted photons efficiently, it is essential to create a very large conic volume with optical setup. Alignment and focusing must be done perfectly before the experiment starts, since intensity of emitted photons is very low [33]. In addition to focusing and alignment, chromatic aberration should be kept in mind since emitted photons have a wide spectrum range [48], [49]. Geometry used by Rendell et al. [50] to calculate the localized surface plasmon modes, the calculated angular distribution of intensity is shown **(Figure 4.2)**.

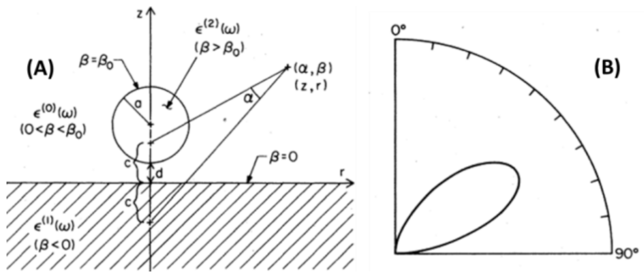

Figure 4.2: Geometry used by Rendell et al. [50] to calculate the localized surface plasmon modes(A), the calculated angular distribution of intensity(B)

In a typical experiment, the ratio of photon creation per tunneling electrons is of the order of 10^{-4} photon/electron [33]. We can make approximate calculation of the intensity we should measure. We start with the current, 1A≈$6,24x10^{18}$ electrons/second. If we scan the surface with 1nA, it means $6,24x10^{9}$ electrons/second. If we multiply this with the rate of photon emission per electron, the result for 1nA tunneling current is $6,24x10^{5}$ photons/second. Detection frequency depends on detector but let's assume 1 kHz. The result is 624 photons/ms, which means when optical setup is perfectly working, detector should be able to detect 624photons/ms. This is a very rough approximation but gives idea about how low the photon intensity is. The first challenge is to collect the emitted photon as much as possible and measure with highest sensitivity. Considering these parameters, one can study on the effects of other parameters such as bias voltage [48], collection angle [51], tip shape [49] etc.

There are three different methods to collect the emitted photons from tunneling junction; mirrors, lens, fibers. The advantage of using mirrors is focus length of the mirror does not change with respect to wavelength. In addition to this, absorbance to reflectance ratio of mirrors is very low. On the other hand, it is hard to align mirrors to tunneling junction due to mechanical problems. For our system, it is easier to align and focus lens to tunneling junction. Lens creates bigger conic volume to collect the emitted photons compared to fibers do. The disadvantage about lenses is photon absorption and chromatic aberration. Chromatic aberration is the failure of the lenses to focus light beam of different wavelength to the same convergence point. It is because refractive index of lens changes with respect to the wavelength.

Considering these advantages and disadvantages of optical components, we had setup two different versions of collection system. One consists of two lens and detector and the other one has one lens, one mirror and fiber. In this chapter, we will present the advantages and disadvantages of both different systems and investigation of photon emission from tunneling junction.

4.2 Experimental Setup

Photon Emission from STM was observed from tunneling junction by placing a photomuliplier tube close to tunneling junction [14]. Considering the photon source as the tunneling junction which is about 1 nm spacing between tip and sample, the light source is a single point light source. There is very little tolerance for alignment and focusing to collect the emitted photons from surface. System is very sensitive of positioning. If a photomultiplier tube with a large active area is placed close to tunneling junction, it is easy to detect emitted photons but if there is a collective optical system before detector, it is not an easy challenge. In our system we placed a collective optical system to collect emitted photons and deliver to photo detector **(Figure 4.3)**.

There is a photon collector head to collect emitted photons from tunneling junction. This optical system can be positioned independently from STM head to isolate STM from outside vibrations **(Figure 4.3)**.

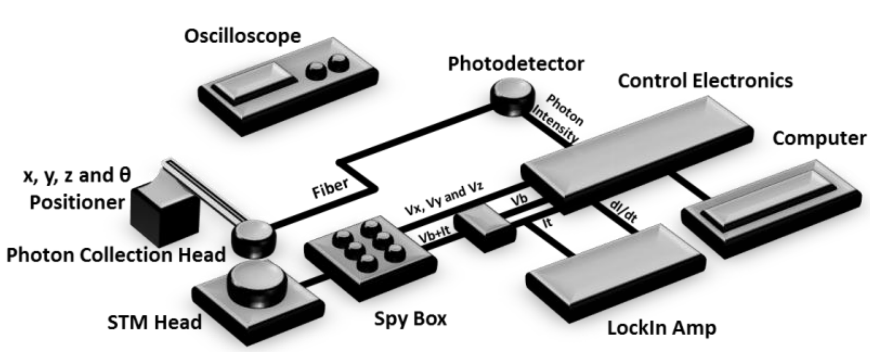

Figure 4.3: Schematic representation for experimental setup

The alignment and focusing of photon collection head to tunneling junction is done by micro positioner in x,y and z direction and θ, ϕ angle. The photodetector can be placed on the photon collection head or collimated light can be delivered to photodetector with a fiber. Photodetector output is plugged to control electronics, so that we can measure photon emission simultaneously with surface topography imaging, or spectroscopy **(Figure 4.4).**

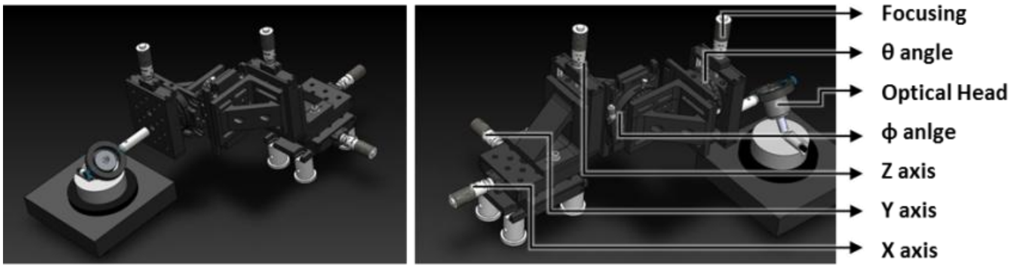

Figure 4.4: CAD drawing of x,y,z axis and θ and ϕ angle positioning system

In our system we are using an aspherical lens to collimate emitted photons from surface. Aspherical lenses are mostly used to focus a laser spot with 1-5mm diameter into single mode fibers. They have a unique surface compared to other types of lens. The main and important reason to choose aspherical lens is to reduce spherical aberration and other optical aberrations. This is very important for optical spectroscopic measurements since spherical aberration and other optical aberrations will directly affect the intensity of light at different wavelengths. In addition to that, aspherical lens can focus larger diameter of incoming light in shorter focal length than spherical lens. We can compare commercially available Thorlabs spherical lenses and aspherical lenses. A spherical lens with focal length of 10 mm, has clear aperture of 6 mm. An aspherical lens with focal length of 8mm has clear aperture of 8mm. This unique design makes it possible to focus larger incoming light to a small point. The opposite optical path is also valid. Light coming from a very small point can be collimated by these lenses **(Figure 4.5)**.

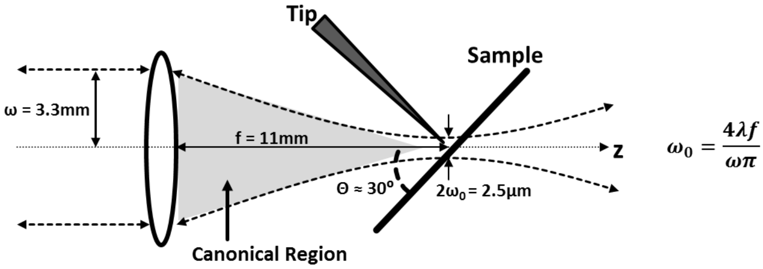

Figure 4.5: Gaussian Beam Concentration in Tunneling Junction

We are using aspherical lens with focal length of 11mm (*f=11mm*) and clear aperture of 6.6mm (*ω=3,3mm*). If we apply the formula for λ=600nm, **(4.1)**

$$\omega_0 = \frac{4\lambda f}{\omega\pi} = \frac{4\times 600nm\times 11mm}{3{,}3mm\times\pi} \cong 2{,}5\mu m \quad \textbf{(4.1)}$$

We calculate the diameter of the spot on focal length ω_0 is 2.5μm for our system. In the region with diameter of 2.5μm the photon emission will follow the optical path mentioned on the figure. We don't need to move the optical system to scan the surface simultaneously with STM tip, because the maximum scan area of tip in our STM head is 400x400nm which is in our collimated spot range.

We are aligning the optical system at the beginning of the experiment and measure the photon emission during surface scan. As it was already mentioned, aspherical lenses are capable of working with smaller focal length with larger clear aperture than spherical lenses. It is desired to approach to tunneling junction as much as possible with wider clear aperture because this will increase the volume of canonical optical path between tunneling junction and lens. The bigger canonical shape means more photons will be collected. We have mechanical limitations to approach to tunneling junction. Design of STM head does not let us approach more than 10mm.

Design of the photon collection head was first realized on 3D Computer Aided Design (CAD) to be sure about how much closer we can get with optical system on STM head and also to be sure about required optical components and accessories. We had copied the design of STM head and used it to realize the setup at first on computer. There was no time and money to waste so, these drawings helped us to choose the best optical components, positioners and accessories for our system **(Figure 4.6).**

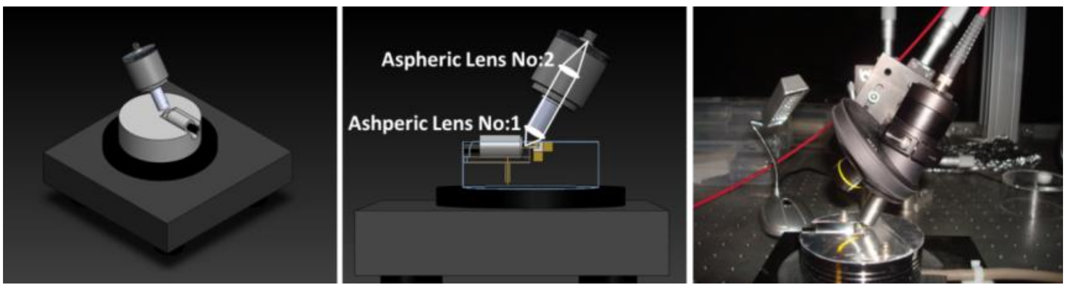

Figure 4.6: 3D CAD drawing of photon collection head with two lenses, estimated photon path and realization of optical setup version one

We made two versions of setup. First version consists of two lenses; first lens is focused on tunneling junction (figure 4.2.4). It is used to collect the light beam from a single point light source and parallelize incoming light beam. The second lens is focused on to the fiber or photo detector. It is used to collimate this parallelized light beam into a fiber or a photo detector **(Figure 4.7)**.

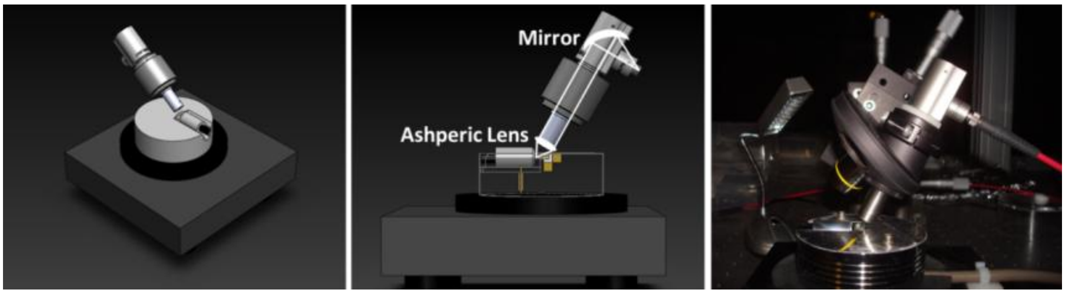

Figure 4.7: 3D CAD drawing of photon collection head with a lens and a mirror, estimated photon path and realization of optical setup version two

The second version of the setup consists of one lens and one mirror (figure 4.2.5). First the lens is focused on tunneling junction and parallelizes the incoming beam. The mirror is focused on fiber output of the system and collimates the parallelized light beam into fiber. The fiber delivers the incoming beam to the photo detector. The advantage of using mirror for collimating incoming beam is the focal length of mirrors does not change with respect to wavelength of light. While collimating light into fiber, we have very little tolerance to focus. The change in intensity with respect to wavelength due to this property of lenses will directly affect our results and give us wrong information from the experiment **(Figure 4.8)**.

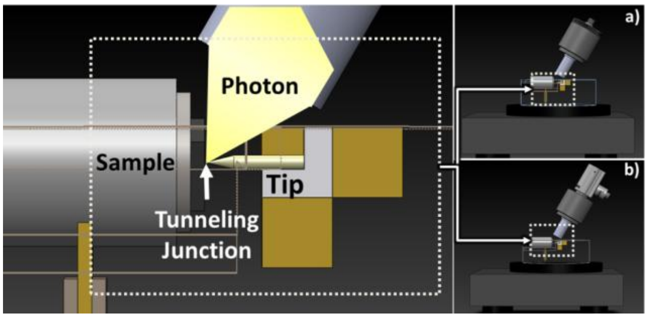

Figure 4.8: 3D CAD drawing of tunneling junction and estimated photon emission path from tunneling junction.

In both versions, it is hard to align and focus the system without looking at tunneling junction through the system. We add an ocular right after the first lens and look at the tunneling junction with eye. We focus the first lens onto tunneling junction. After aligning first lens we remove the ocular and place second lens on the other side of the lens tube. The second lens doesn't need to be aligned to tunneling junction because it will be already aligned in the middle of lens tube as seen on the 3d CAD drawings of optical setup. We are just measuring the distance between the fiber adapter and lens with a ruler **(Figure 4.9)**.

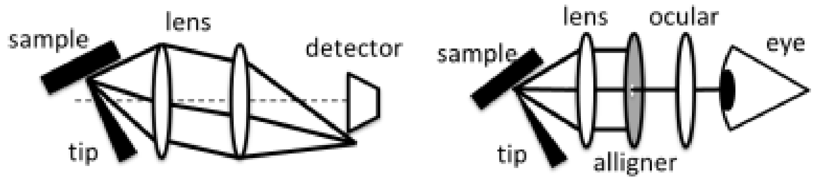

Figure 4.9: Alignment error and a simple correction method.

If the system is not aligned perfectly, measured photon intensity will be too low even close to zero. We made a little aligner for the system as shown in the figure 4.2.8. There is a very small hole in the middle of aligner. This hole let us have the second point for alignment (figure 4.2.7). We are drawing an imaginary straight line passing through two points. First point is tunneling junction and second point is the middle of this aligner **(Figure 4.10)**.

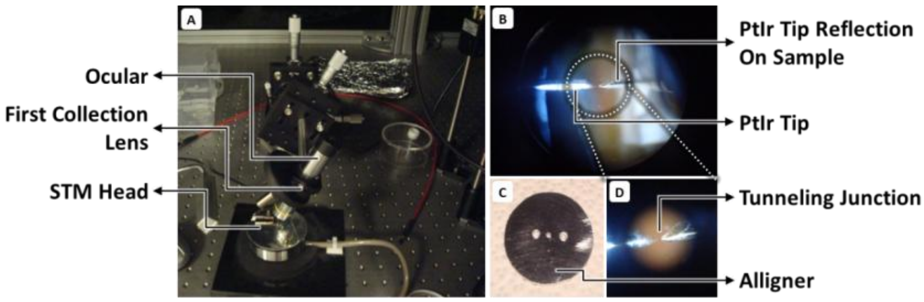

Figure 4.10: Alignment with ocular before starting the measurement(A). the tip and its reflection on the surface(B). When the aligner (C) is placed after the first lens it is easier to align (D).

The measurements should be done in isolated conditions from any external light sources. We visualized isolation cage at CAD drawings and constructed the framework with aluminum profiles and covered with plexiglas which has 100% opacity. Light intensity inside cage is almost zero and it is a very small probability for any external light beam to follow the optical path and affect the measurement **(Figure 4.11)**.

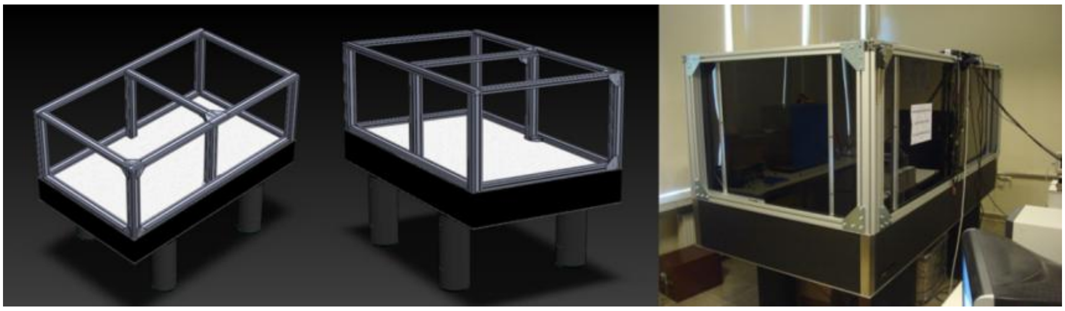

Figure 4.11: CAD drawing and realization of light isolation box

After preparing the system for the experiments we had realized the system isolated from external vibrations and light sources. In figure below the realized setup is shown **(Figure 4.12)**.

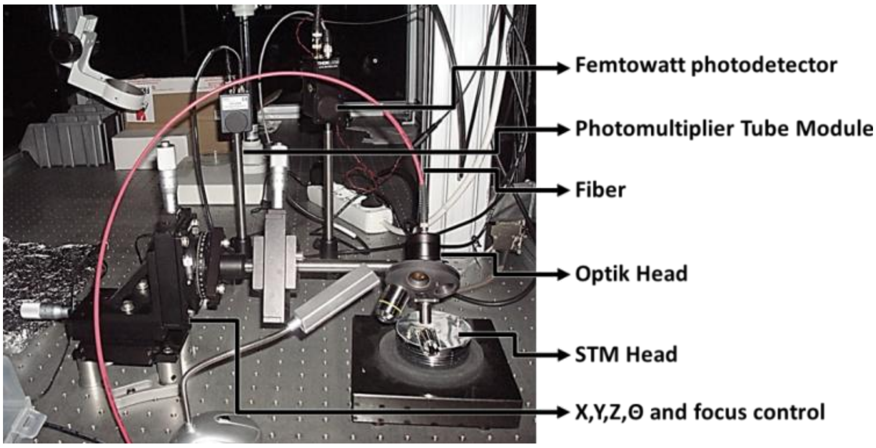

Figure 4.12: Realization of experimental Setup

4.3 Photon Emission from STM

After realizing the setup, it took a lot of time to observe the photon emission from tunneling junction. We started experiments with photomultiplier tube (PMT) to measure photon emission. Photomultiplier tubes are used for very low intensity light measurements and photon counting systems for their high sensitivity and high speed properties [52].

Our PMT was a budget friendly PMT module from Thorlabs (PMM02). This PMT module has 10μs rise and fall time. In other words detection frequency of light beam is 100 kHz. As it is shown on the graph below, the signal output of PMT is very sharp peaks. Our STM control electronics did not let us measure the output signal. To measure such a signal from PMT, control electronics must be much faster than 100 kHz or PMT output should be slowed down with a low pass filter **(Figure 4.13)**.

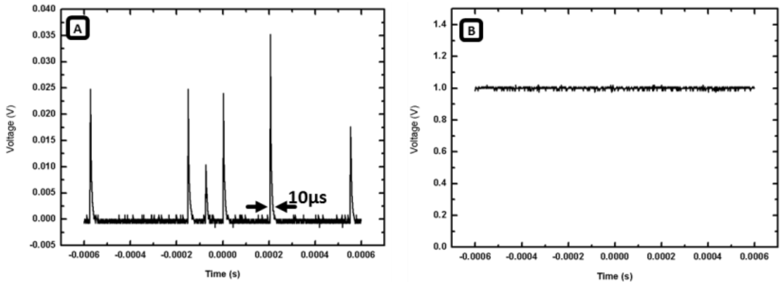

Figure 4.13: PMT output signal (A) and power supply with batteries output (B)

Another problem of PMT module is its dark count rate. On the graph above figure 4.3.1 (A), these peaks are measured when the PMT input is totally closed and there is no signal input. These peaks are not periodical and do not have certain amplitude, because of this we cannot use any filtering method to cancel dark counts perfectly. At first we thought they were because of power supply noise. We constructed our power supply with batteries to eliminate power supply noise due. Despite this, there were still those random peaks. These peaks are called dark counts. We tried to filter them using 100 kHz low pass filter but this time technique also didn’t work. The amplitude of input signals is very low and they are not distinguishable. We tried to detect the emitted photons with femtowatt photodetector from Thorlabs.

The first successful experiment of photon emission from stm obtained with our system created big excitement and motivation. We used rough Au sample to observe photon emission from surface system. The sample was prepared by thermal evaporation on mica surface under vacuum conditions. The thickness of gold on mica is approximately 500nm. As it is shown on the figure 4.3.2, surface topography and photon map have a correlation as it is expected to be. On the other hand, in this image, tunneling current and photon map also have correlation like surface topography. The correlation of photon map and tunneling current is proposed as the effect of tunneling current on intensity of photon emission from the surface.

On tunneling current map, as the color gets darker, tunneling current gets higher. At these dark points, the photon emission is higher too. When tunneling current gets higher, photon emission is getting higher. This is an expected result. We are working with constant tunneling current mode but depending on the scan speed, sometimes the response speed of feedback mechanism is slower than scan speed. Tunneling current can increase at edges of Au islands until feedback mechanism moves tip upwards. This is also valid for other samples rather than Au.

On the image, one of the Au islands is marked. The right side and left side of the same island is investigated. When STM is scanning surface from left to right (forward), the tunneling current gets higher on the left side of the island and photon emission is observed from left side of the island. When STM is scanning surface from right to the left (backward), the tunneling current gets higher on the right side of the island and photon emission is observed from right side of the same island. **(Figure 4.14)**.

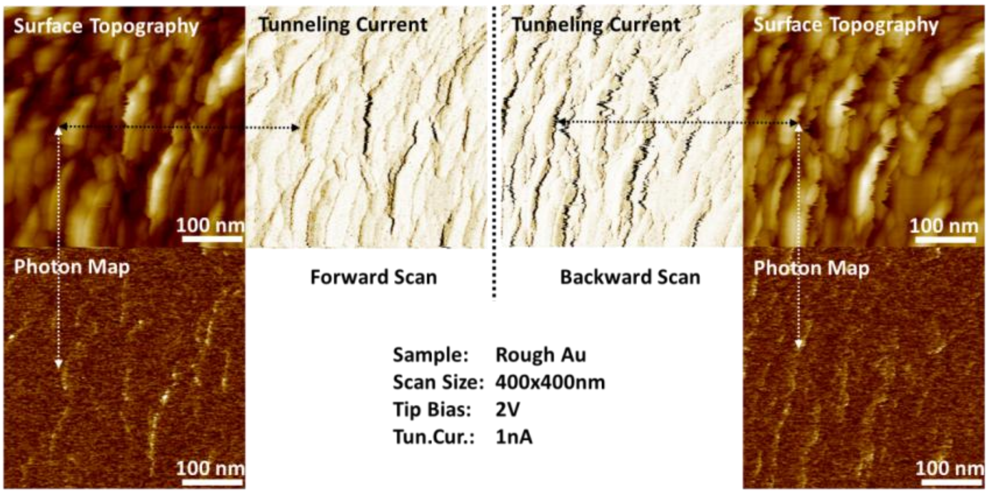

Figure 4.14: First successful photon emission experiment with our system.

This was only beginning and first successful experiment but there were very much information on the results. The correlation between tunneling current and photon emission is observed as a beginning. Before we continue our experiments we had to make a decision whether we should continue with Femtowatt photodiode photodetector or PMT **(Figure 4.15)**.

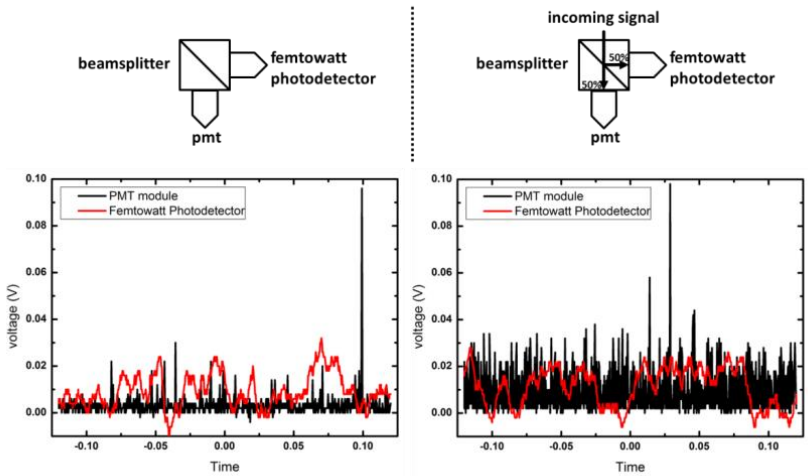

Figure 4.15: PMT module and Femtowatt Photodetector comparison

When we compare the sensitivities of both PMT module and Femtowatt Photodetector, we see that the average output for both of them is equal. We used a beam splitter with 50-50 splitting. At first, the cover of beam splitter was closed and there was no signal passing through the detectors. The average dark currents measured with an oscilloscope at both two detectors were equal. Low intensity light beam was sent into beam splitter and 50% of incoming signal was sent to PMT and 50% of incoming signal was sent to femtowatt photodetector. The average signals measured from both two detectors were equal.

These results show us that sensitivities for both were the same but our electronics were not capable to detect the sharp peaks of photomultiplier tube module. We had tested the photomultiplier tube and femtowatt photodetector together with 50-50 beam splitter to be sure about when the system is working if we can detect the photon emission with PMT and femtowatt photodetector together. We observed the photon emission from tunneling junction with femtowatt photodetector but we couldn't observe the photon emission with PMT module. After the results we obtained with PMT module and Femtowatt photodetector we decided to continue our experiments with Femtowatt photodetector **(Figure 4.16)**.

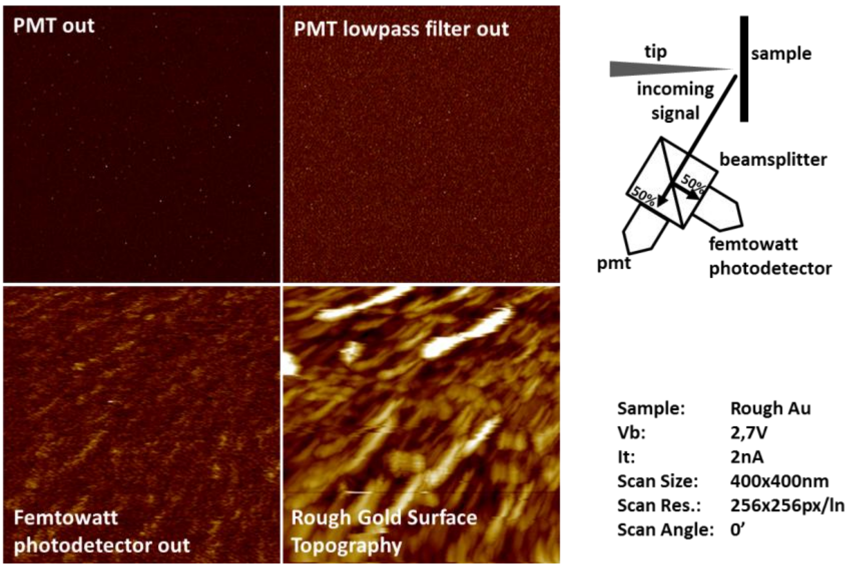

Figure 4.16: PMT module and Femtowatt Photodetector comparison

In some experiments we could observe the photon emission from tunneling junction but sometimes we couldn't observe the photon emission from tunneling junction with the same system and same parameters. When we read the previous works about the photon emission from tunneling junction experiments and calculations, it is mentioned as, the energy and intensity of emitted photon depends on the shape of the tip. As the tip gets sharper, photon emission gets higher and energy of emitted photons increases [53] **(Figure 4.17)**.

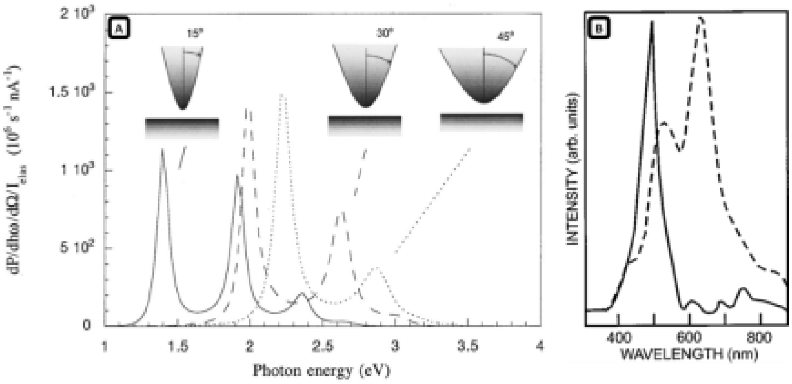

Figure 4.17: The correlation between the tip sharpness and photon emission (A) simulation results and (B) experimental results with two different tips [53].

When we understand the correlation between the tip and photon emission, we decided to focus on finding the best tip and tip preparation method for our system. PtIr tip is a very widely used STM tip in ambient conditions. The shape of the top of the tip is very important parameter for photon emission but it is not an easy challenge.

We are using PtIr tip produced by mechanically cutting 250µm PtIr wire. Unfortunately it is not possible to control the shape of the tip by cutting. In some cases, tip is cut very sharp and we can measure the photon emission very well, sometimes it is not cut very well and we cannot measure photon emission however we can image the surface very well and sometimes we cannot image the surface very well but we observe photon emission (figure 4.3.6). Actually we are not sure if the main reason for not observing the photon emission is because of tip. There can be any other reason for not observing the photon emission **(Figure 4.18)**.

Figure 4.18: Mechanically cut PtIr tip can be either a good tip or bad tip for Photon Emission-STM experiments

In the case of figure 4.3.7, we can clearly see the gold nano islands on the surface but we cannot see the photon emission from the surface. We assume that we are nearly focused on the tunneling junction because we align and focus the optical head with the same method every time. The reason could be the shadow effect of the tip because of mechanically cutting. Good tip for STM imaging was not good for photon emission from STM experiments all the time **(Figure 4.19)**.

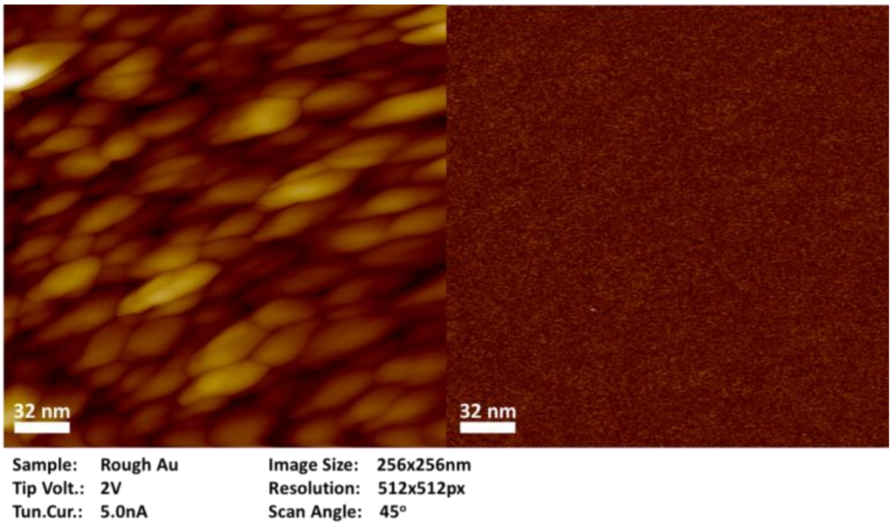

Figure 4.19: However tip is good for imaging, we couldn't observe the photon emission from Au islands.

Good tip for STM imaging was not good for photon emission from STM experiments all the time **(Figure 4.19)**. On the other hand, the opposite of this is also valid. Some tips are very good for photon emission but good not surface imaging **(Figure 4.20)**. We cannot observe the gold island on the surface on the image but we can see the photon emission. Some parts of the gold surface are shining.

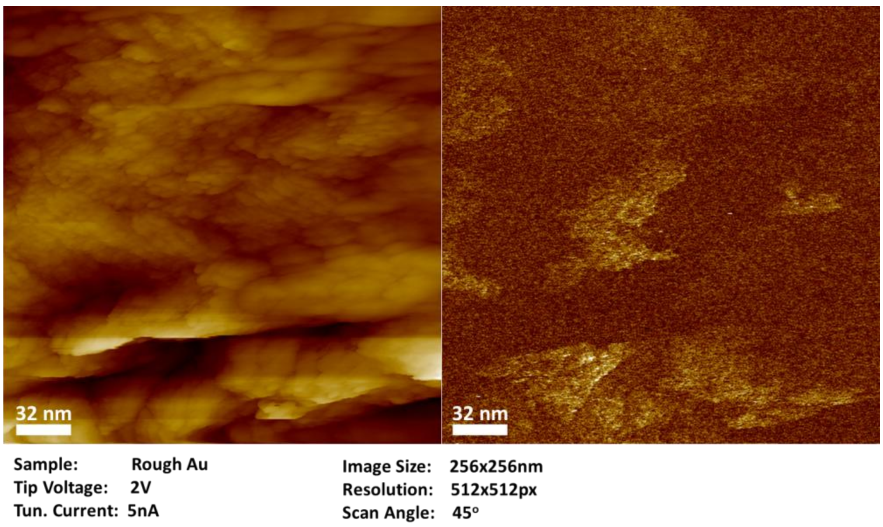

Figure 4.20: However mechanically cut tip is not good enough to image surface topography very well, we can still observe photon emission related to topography

We are not 100% sure about the reasons behind these results. As you can see the tip can be very good for PE experiments or topography studies or for both of them. On the next sample, **(Figure 4.21)** tip is good enough to observe both gold islands and photon emission from surface.

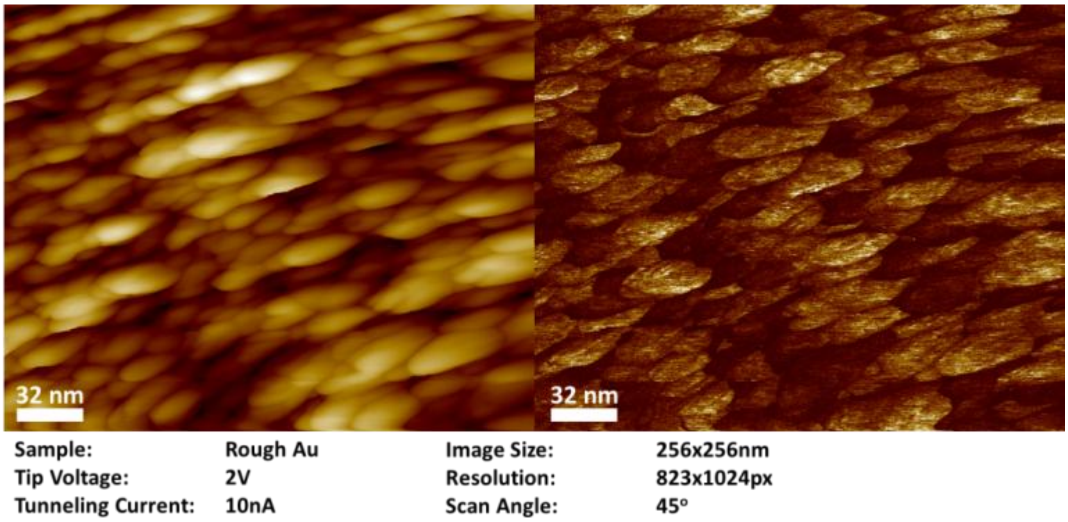

Figure 4.21: topography (A) and photon emission map (B) is observed with mechanically cut tip. Tip is good enough to observe both gold islands and photon emission from surface

Another reason for not observing photon emission from tunneling junction can be tip shadow. The shape of top of tip can shadow emitted photons despite it is sharp on the top and we can image the surface perfectly. When we investigate the shape of the top of the tip its structure is sharp on the top but it is blunt around the top **(Figure 4.22)**.

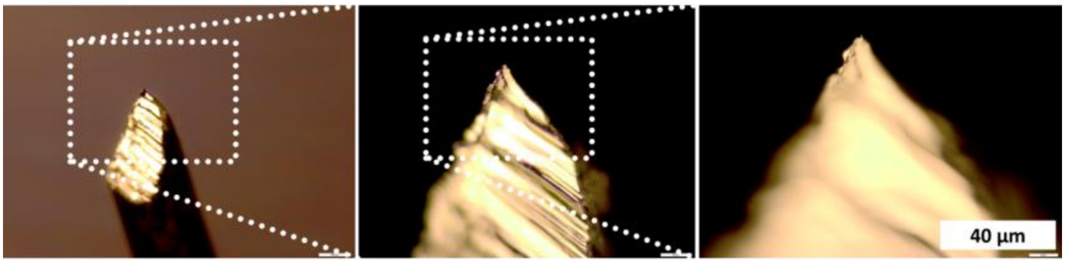

Figure 4.22: Image of mechanically cut PtIr tip

We had tested this this effect. We started to measure photon emission from one side of tip and we couldn't observe any photon emission when we turned tip to the other side, we could observe photon emission **(Figure 4.23)**. Mechanically cut tip surface is observed with an optical microscope.

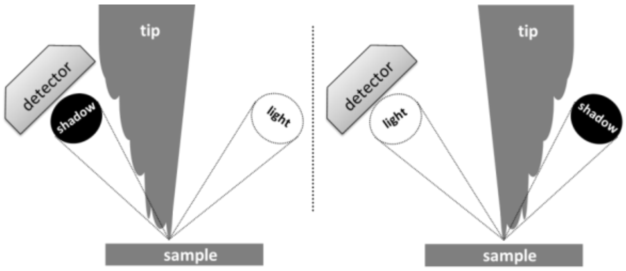

Figure 4.23: Tip shadow depending on the cut side of tip.

We had worked on chemically etching the tip but it still needs to be developed. Imaging the surface at low bias voltages gives us good surface topography image but when we increase the bias voltage the image becomes blurred. It looks like, the top of the tip still remains blunt which causes tunneling occur from a wide area. This will reduce the resolution of image. This effect is shown on the images taken from the same surface area but different bias voltages **(Figure 4.24)**.

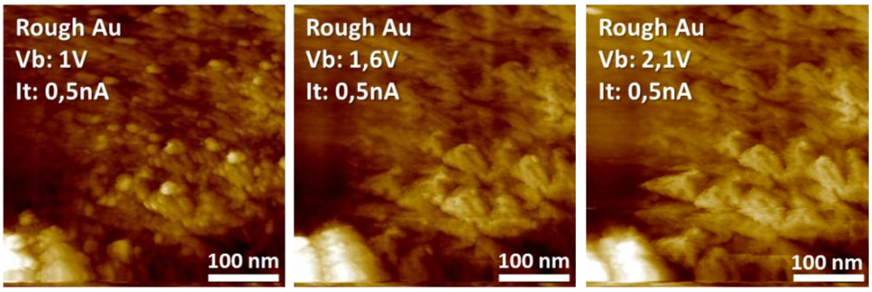

Figure 4.24: Chemically etched PtIr tip and images on same area, different bias voltages were applied

The second reason for our prediction was the experiences we had with some of the chemically etched tips. As we increased the bias voltage, tunneling current was increasing also but it was going beyond the set value despite feedback mechanism retracts the tip. The software was showing this fact as tip is in contact with the surface since tunneling current rises above the set value. In an STM system when bias voltage is increased, tunneling current increases and feedback mechanism retracts tip from surface and keeps the tunneling current constant at set value. The range of z axis piezo is limited to 408nm in our system and tip cannot be retracted beyond this limit. The problem was the etching process was not well done and top of the tip was blunt a lot. When we increase the bias voltage tunneling occurs from many points of tip and tunneling current increases and goes beyond the set value. Feedback mechanism retracts the tip but still cannot set the tunneling current back to set value. We observed this by scoping the tunneling current and Vz **(Figure 4.25)**.

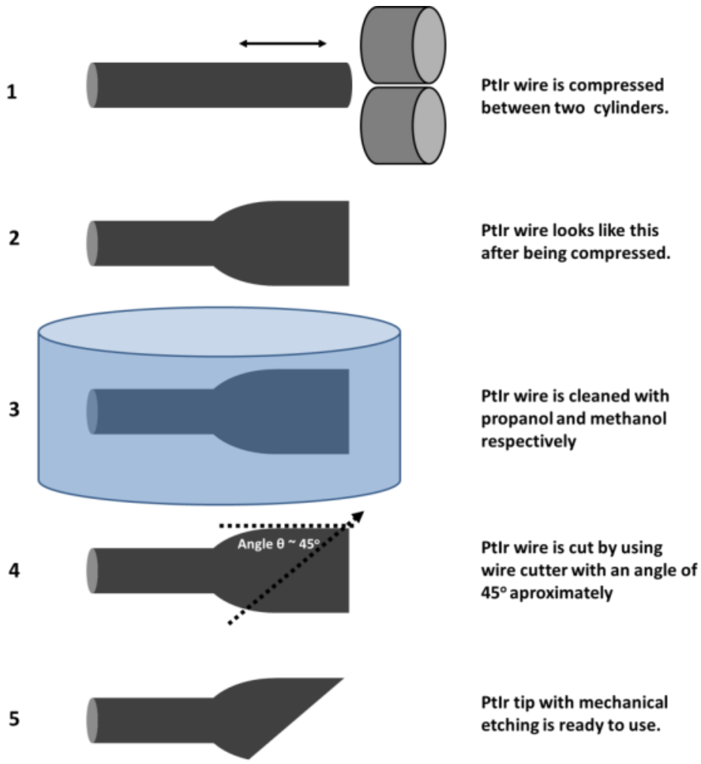

Figure 4.25: Our method to prepare mechanically cut tip.

We also worked on controlling the tip shape with mechanically etching. We had developed a new method for preparing tip (figure 4.3.13). When we compare the mechanically cut tip and our way of mechanically cutting, we could observe the difference even on optical microscope (figure 4.3.13). We couldn't observe any photon emission from tunneling junction with blunt tip but sharp tip gives us good results **(Figure 4.26)**.

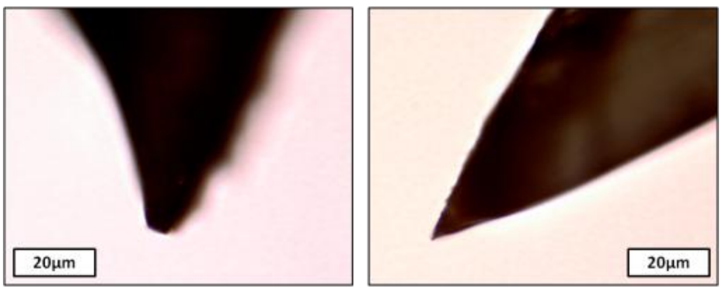

Figure 4.26: Comparing mechanically cut STM tip with usual way (A) and our method (B). Experimental results and this image shows that we are on a good way.

We had tested our new mechanically cut tips with our new method and the results looks like tips are good for surface imaging and studying photon emission. As seen on figure 4.3.15, the surface topography was imaged very well and photon emission is also mapped very well. This shows that our method is working for now, since our main focus of our project is not finding a new method to prepare good, sharp tip for PE-STM, we did not spent much time on this method and investigating the results **(Figure 4.27)**.

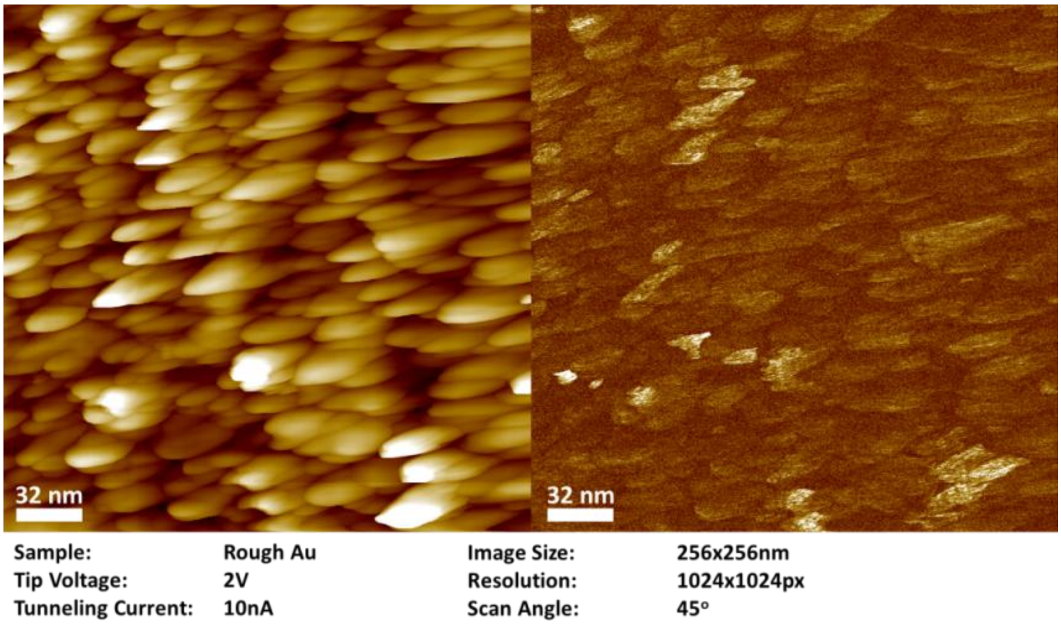

Figure 4.27: New tip etching method was tested and looks promising

Another problem we deal with was the dust and humidity sticking on the Gold surface. We could get rid of humidity and dust on the gold surface by applying approximately 1 Bar of He gas on the surface for a minute **(Figure 4.28)**.

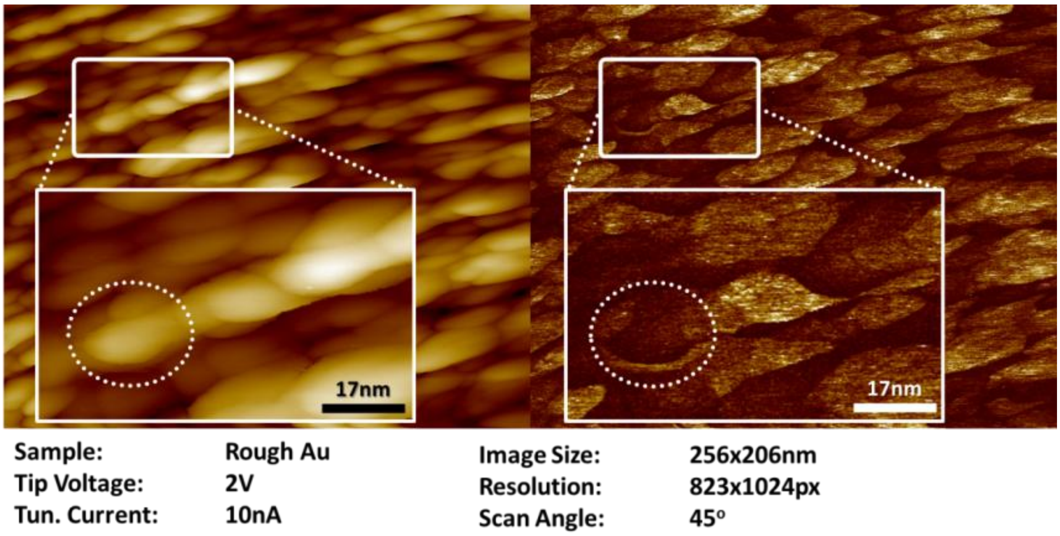

Figure 4.28: On some of the Au islands, photon emission is very high but on some of them there is no photon emission. As shown in circle, the Au island on the top emits no photon but below that Au island, the photon emission is very high

Understanding the reasons and affecting parameters to photon emission from surface system is too complicated. There are so many parameters that change the photon emission intensity and spectrum, such as ambient conditions, surface humidity, surface topography, tip shape, metal thin film thickness etc. Unfortunately these are all uncontrollable parameters for our setup. On some of the Au islands, we observed photon emission very high but on some of them there was no photon emission. As shown in figure 4.3.16, in the circle, the Au island on the top emits no photon, it is totally dark in photon map but below that Au island, photon emission is very high. The same case is valid for many Au islands on the image.

We can study on the correlation of surface topography and photon emission over a limited area and time. Mostly we can look at a single photon map, since we cannot be sure about the same conditions are satisfied. The shape of the tip can change as we mentioned in previous chapter in **(Figure 4.29)**. The shape of the tip is very important for photon emission [49].

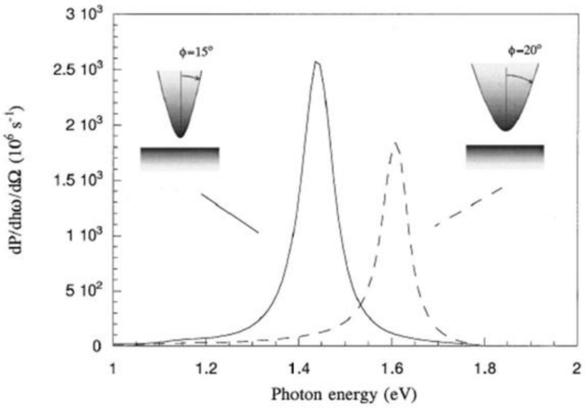

Figure 4.29: When the shape of the tip changes, the photon emission intensity and spectrum changes also.

When we look at the surface topography and photon map cross section, in some cases, we can say that if the top of the gold island is sharper **(Figure 4.30)**, the photon emission gets higher. As we had mentioned before, we should break the symmetry of the surface plasmons. Otherwise, due to the evanescent field and non-radiative nature of surface plasmons, power (photons) cannot propagate away from the surface.

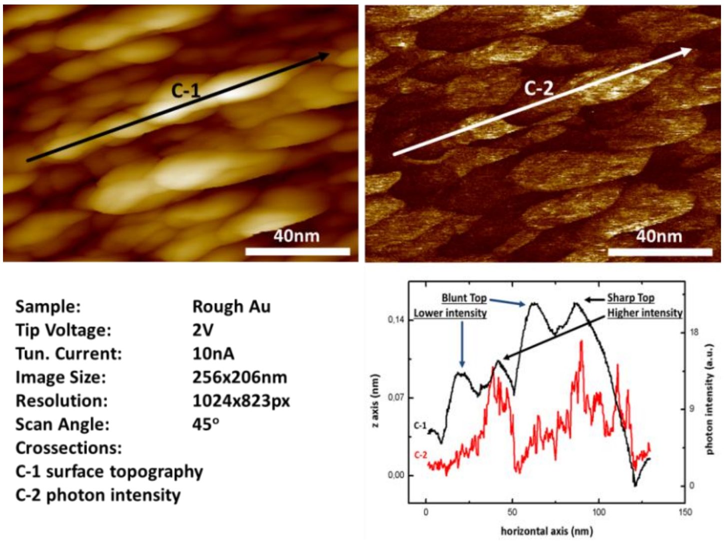

Figure 4.30: Cross section of photon emission and surface topography, the sharper Au Island gets, the higher intensity photon emission occurs.

We had obtained many important results with our system but still there is lots of work to do and lots of questions waiting for an answer. The relation between the surface topography and photon emission map is not very simple to understand and explain. In some regions on the surface, the photon emission increases when the height of Au island is increasing rapidly **(Figure 4.31)**.

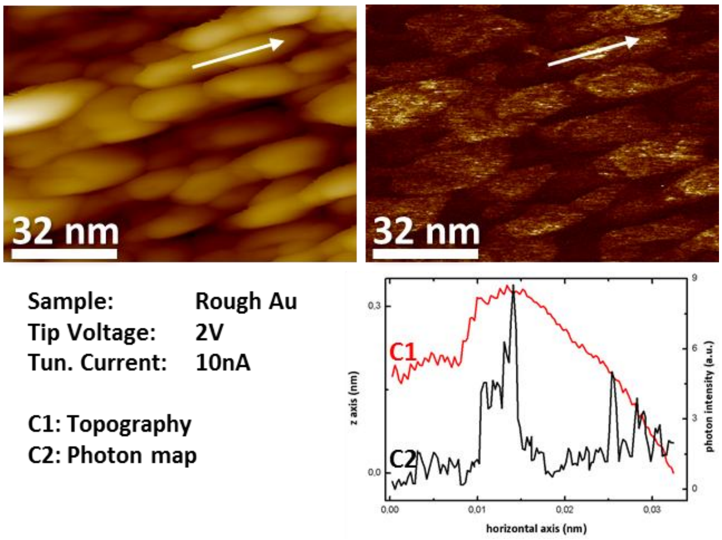

Figure 4.31: Rapid topological changes increase the photon emission.

If the height of Au island is increasing sharp, or the surface topography is changing very rapidly, photon emission intensity is high but if surface topography is increasing slowly, photon emission is getting lower **(Figure 4.32)**.

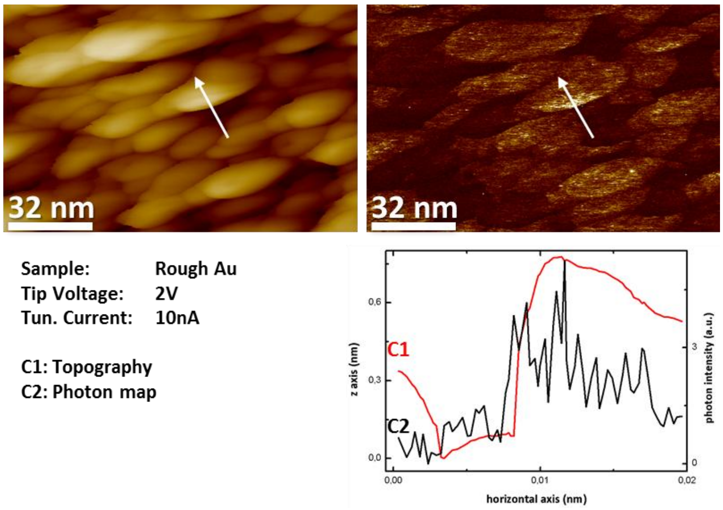

Figure 4.32: Rapid topological changes increase the photon emission.

The experimental results of Dawson et.al show us that the photon emission should be very familiar to the surface topography. Their results are very different from our results. Every single gold island is shining in their results. Their results raises many questions. As shown in the circle, it looks like the photon emission depends on the thickness of the gold film rather than surface topography [54] **(Figure 4.33)**.

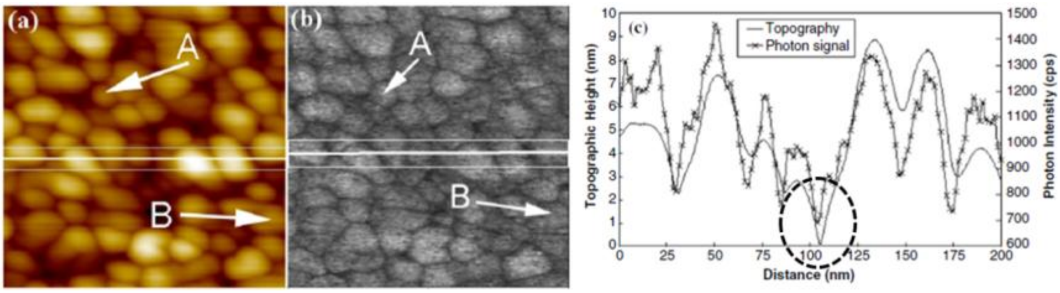

Figure 4.33: Experimental results represented by P Dawson et.al. [54].

In our results, we see that some gold island shines very bright but the neighbouring gold islands do not emit any photons. The question about this result is what makes it so special to shine very bright **(Figure 4.34)**. It is hard to understand and explain why on some islands the photon emission is very high and on some of them it is close to zero.

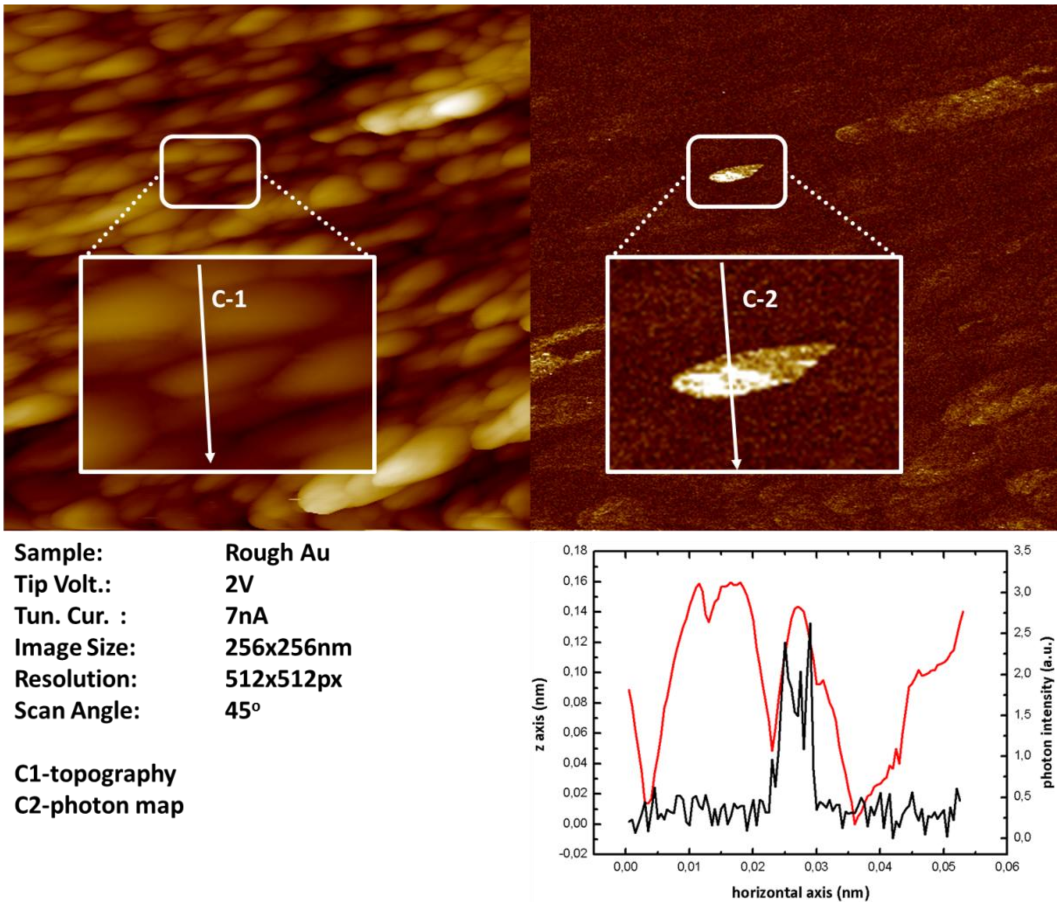

Figure 4.34: Photon emission from some Au islands is much more than others. What makes that small Au island so special that it is very bright on photon map.

We decided to take a closer look and take a higher resolution image. We zoomed into the shining Au island to look closer and to study spectroscopy on the shining Au island **(Figure 4.35)**. This is the best way to study spectroscopy on the surface. We tried to study spectroscopy on the shining Au island but as seen on the graphs our system did not let us take a good data.

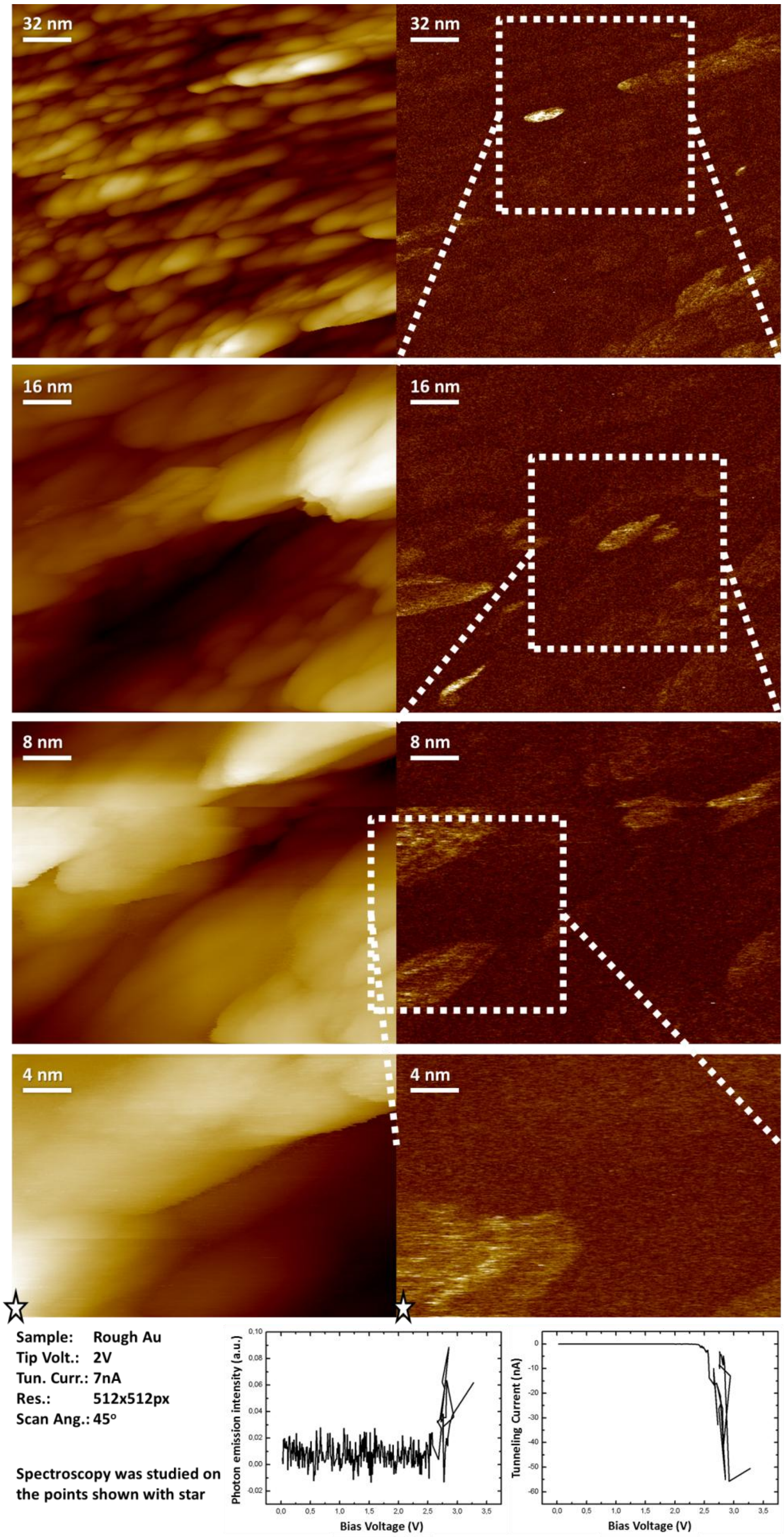

Figure 4.35: We zoomed into the shining Au island to look closer and to study spectroscopy on the shining Au island.

5. CONCLUSIONS AND FUTURE WORK

In this work, we had designed and constructed a scientific grade, experimental setup for observing photon emission from scanning tunneling microscope. We modified a student educational purpose STM system, integrated our scientific grade control electronics and construct our scientific grade PE-STM system. By using this electronics, we added more options, more input and output channels and by using these extra channels, we had created more freedom for measurements.

We started with reverse engineering for commercially available student educational purpose STM system to integrate into our control electronics. We investigated the basic working principles, electronics and mechanical system of this Scanning Tunneling Microscope. We are still having some troubles about the hardware and software.

This configuration of the system enables us to make a good start on working on photon emission from tunneling junction. We had observed the correlation between the surface topography and emitted photon intensity. When there is a rapid change in surface topography, the symmetry of surface plasmons is broken and cannot prevent the power loss so the photon emission is observed. We also worked on a new STM tip preparation method.

For the future works, it is already planned to study different surface systems, nanostructures such as Quantum Dots or nano wires. The system is also suitable to add more measurements such as monochromator to do optical spectroscopy simultaneously with the surface scan.

REFERANCES

[1] E. Abbe, "Beitrage zur Theorie des Mikroskops und der mikroskopischen Wahrnehmung," vol. 7, no. 413-420, 1873.

[2] E. Ruska, "The development of the electron microscope and of electron microscopy," vol. 59, no. 627-638, 1987.

[3] M. S. R. J. R. B. R. A. S. H. R. S. L. Kipp, "Sharper images by focusing soft X-rays with photon sieves," vol. 414, no. 184-188, 2001.

[4] W. D. M. L. D.W. Pohl, "Optical stethoscopy: Image recording with resolution λ/20," vol. 44, no. 651-653, 1984.

[5] B. H. D. P. L. Novotny, "Implications of high resolution to near-field optical microscopy," vol. 71, no. 341-344, 1998.

[6] F. K. A. K. R. G. H.G. Frey, "Enhancing the resolution of scanning near-field optical microscopy by a metal tip grown on an aperture probe," vol. 81, no. 5030-5032, 2002.

[7] E. S. E. a. W. A. C. G. J. Rosasco, "The Analysis of Discrete Fine Particles by Raman Spectroscopy," vol. 29, no. 394-404, 1975.

[8] P. H. A. M. M. Fleischmann, "Raman spectra of pyridine adsorbed at a silver electrode," vol. 26, no. 163, 1974.

[9] Y. S. V. D. R. Z. R.M. Stöckle, "Nanoscale chemical analysis by tip-enhanced Raman spectroscopy," Vols. 131-136, 2000.

[10] B. P. J. Steidtner, "Tip-Enhanced Raman Spectroscopy and Microscopy on Single Dye Molecules with 15 nm Resolution," vol. 100, no. 236101, 2008.

[11] R. D. W. J. a. S. F. Young, "The Topografiner: An Instrument for Measuring Surface Microtopography," vol. 43, no. 7, 1972.

[12] H. R. C. G. E. W. G. Binnig, "Tunneling Through a Controllable Gap," vol. 40, no. 2, 1982.

[13] C. C. J., Introduction to Scanning Tunneling Microscopy, OXFORD UNIVERSITY PRESS, 1993.

[14] B. R. J. C. R. S. J.K. Gimzewski, "photon emission with the scanning tunneling microscope," vol. 72, no. 497, 1988.

[15] R. G. a. W. S. R. Berndt, "Atomic Resolution in Photon Emission Induced by a Scanning Tunneling Microscope," vol. 74, no. 1, 1995.

[16] K. A. D. T. e. a. L. Theresa, "Scanning Tunneling Luminescence of Individual CdSe Nanowires," vol. 7, no. 16, 2011.

[17] P. R. D. A. C. S. D. A. a. H. M. S. Alvarado, "Luminescence in scanning tunneling microscopy on III-V nanostructures," vol. 9, no. 409, 1991.

[18] M. K.-J. J. M. H. C. P. L. S. W. S. a. M.-E. P. U. Håkanson, "Photon mapping of quantum dots using a scanning tunneling microscope," vol. 81, no. 23, 2002.

[19] J. v. d. L. M. Romero, "Luminescence of quantum dots by coupling with nonradiative surface plasmon modes in a scanning tunneling microscope," vol. 80, no. 115432, 2009.

[20] A. S. V. N. P. A. M. P. V. W. V. B. M.R. Hummon, "Measuring charge trap occupation and energy level in CdSe/ZnS quantum dots using a scanning tunneling microscope," vol. 81, no. 115439, 2010.

[21] A. A.P., "Semiconductor Clusters, Nanocrystals, Quantum Dots," vol. 271, no. 933–937, 1996.

[22] C. Chen, Introduction to Scanning Tunneling Microscopy, Oxford University Press, 1993.

[23] R. WIESENDANGER, Scanning Probe Microscopy, Cambridge Universtiy Press, 1998.

[24] D. Griffits, Introduction to Quantum Mechanics, Pearson Education Inc., 2005.

[25] A. D. T. E. W.L. Barnes, "Surface plasmon subwavelength optics," vol. 424, no. 824-830, 2003.

[26] Z. H. P. B. Gurlu O, "Electronic properties of (2×1) and c(4×2) domains on Ge(001) studied by scanning tunneling spectroscopy.," vol. 93, no. 066101, 2004.

[27] H. J. Z. a. A. v. Houselt, "Scanning Tunneling Spectroscopy," vol. 2, 2009.

[28] J. R. B. G. W. &. Y. F. Z. Sambles, "Optical excitation of surface plasmons: an introduction," vol. 32, no. 173-183, 1991.

[29] S. a. R. Tien-Lai Hwang, "Plasma Radiation from Tunneling Junction," vol. 36, no. 379-382, 1976.

[30] S. John Lambe, "Light Emission from Inelastic Electron Tunneling," vol. 37, no. 923-925, 1976.

[31] P. Johanson, "Light emission from a scanning tunneling microscope: Fully retarded calculation," vol. 58, no. 16.

[32] U. H. L. R. a. V. S. S. Kühn, "Enhancement of Single-Molecule Fluorescence Using a Gold Nanoparticle as an Optical Nanoantenna," vol. 97, no. 017402, 2006.

[33] R. M. a. P. A. P. Johanson, "Theory for Photon Emission from a Scanning Tunneling Microscope," vol. 42, no. 14, 1990.

[34] P. Johansson, "Light emission from a scanning tunneling microscope: Fully retarded calculation," vol. 58, no. 16, 1998.

[35] R. Weisendanger, Scanning Probe Microscopy and Spectroscopy Methods and Applications, cambridge university press, 1998.

[36] O. Z. a. D. W. P. U. Dürig, J. Microsc. 152, 259 , 1988.

[37] B. I. a. S. Ciraci, "theoretical scanning tunneling microscopy and atomic force microscopy study of graphite including tip-surface interaction," vol. 6, no. 2, 1988.

[38] V. E. a. F. Wudi, "Tunneling Microscopy on Various Carbon Materials," vol. 6, no. 2, 1988.

[39] A. B. B.N.J. Persson, vol. 59, no. 339, 1987.
[40] T. Komeda, vol. 78, no. 41, 2005.
[41] M. R. a. W. H. B.C. Stipe, "Single-Molecule Vibrational Spectroscopy and Microscopy," vol. 280, no. 1732, 1998.
[42] J. P. L. Z. H. K. a. A. J. M. N. J. Watkins, "Fiber optic light collection system for scanning-tunneling-microscope induced light emission," vol. 78, 2007.
[43] R. C. F. A. J. B. R. Pechou, "Control of light emission from an STM and surface modifications," vol. 418, 1998.
[44] R. G. W. S. R. Berndt, "Atomic Resolution in Photon Emission Induced by a Scanning Tunneling Microscope," vol. 74, no. 1, 1995.
[45] M. K. V. E. I.I. Smolyaninov, "Emission of Light by the Tunneling Junction of a Scanning Tunneling Microscope," vol. 52, no. 3, 1990.
[46] J. M. a. P. D. M. G. Boyle, "Infrared emission from tunneling electrons: The end of the rainbow in scanning tunneling microscopy," vol. 94, no. 233118, 2009.
[47] R. R. S. a. J. K. G. R. Berndt, "Photon emission scanning tunneling microscope," vol. 9, no. 2, 1991.
[48] J. S. R. S. J. S. J.K. Gimzewskı, "Enhanced Photon Emission in Scanning Tunnelling Microscopy," vol. 8, no. 5, 1989.
[49] S. A. a. R. B. J. Aizpurua, "Role of tip shape in light emission from the scanning tunneling microscope," vol. 62, no. 3, 2000.
[50] R. R. a. D. Scalapino, "Surface Plasmons Confined by Microstructures on Tunnel Junctions," vol. 24, no. 3276-3294, 1981.
[51] R. R. a. D. Scalapino, "Surface plasmons confined by microstructures on tunnel junctions," vol. 24, no. 6, 1981.
[52] H. P. K. E. Committee, Photomultiplier Tubes, Basics and Applications, Hamamatsu Photonics K.K., 2006.
[53] J. A. Apell S. P., "Role of tip shape in light emission from the scanning tunneling microscope," vol. 62, no. 3, 2000.
[54] P. D. a. M. G. Boyle, "Light emission from scanning tunnelling microscope on polycrystalline Au films—what is happening at the single-grain level?," vol. 8, no. 219-226, 2006.

APPENDICES

APPENDIX: There is no appendix for this study.

CURRICULUM VITAE

Name Surname: Mehmet Selman TAMER

Place and Date of Birth: Aydın 1986

Address: Efeler Mah. 1402 Sok. No:3/4 Merkez - Aydın

E-Mail: selmantamer@gmail.com

B.Sc.: Koç University, Physics

Professional Experience:

LOT-QuantumDesign GmbH. Darmstadt, Germany
2012 – (cont.) Regional Sales Manager

- Working as area sales manager in Turkey

Istanbul Technical University Nanoscale Surface Research Laboratories, Istanbul, Turkey
2010 – 2012 Research Assistant and Software Developer, Supervisor: Asst.Prof.Oğuzhan Gürlü

- Worked as Research Assistant at TUBITAK supported project, "Observation of Optical Excitations at Nanoscale Tunnel Junctions."
- Designed and Realized a Photon Emission from Scanning Tunneling Microscope (PE-STM) system and also worked on Si(001) surface preparation methods in UHV system and developed LabVIEW software for the experiments.

OZ Optics A.Ş. İzmir, Turkey
2009 – 2010 Production, Coordination and Marketing Executive Assistant

- Worked as coordinator between OZ Optics Canada and OZ Optics Turkey
- Worked as Assistant of Production and Marketing

Koç University Microphotonics Research Laboratories, Istanbul, Turkey
2005 –2009 Research Assistant and Software Developer, Supervisor: Prof. Ali Serpengüzel

- Worked on experimental setup, software development and theory for microparticle (silicon, ruby, glass, sapphire) spectroscopy (scattering measurements) and electrical properties (I-V characteristics) and control software development for LambdaPhysik LPD3000 dye laser
- Designed and realized a computer controlled and automated spectroscopy system using LabVIEW to control a spectrometer.

OSA (Optical Society of America) Student Chapter Koç University, Istanbul, Turkey

2008 – 2009 President

- Organized photo contest with optical merit.
- Organized solar powered boat race.
- Organized lecturer Dr. Rachel Won's visit to Turkey.
- Attended to the annual frontiers in optics conferences and meeting of OSA chapter leaders at Rochester NY

SPIE (International Society for Optical Engineering) Student Chapter Koç University, Istanbul, Turkey

2007 – 2008 Vice-President

- Organized of solar powered Zeppelin race
- Organized of lecturer Dr. Bahram Javidi's visit to Turkey.
- Translated international OSA and SPIE posters about photonics into Turkish

List of Publications and Patents:

- "Photon Scanning Tunneling Microscopy System for Observing Optical excitations at Nanoscale Tunnel Junctions" Tansu Ersoy, **Mehmeh Selman TAMER**, Oguzhan GÜRLÜ, Nanotr6 Conf., Izmir TR (2010).

- "Photon Scanning Tunneling Microscopy System for Observing Optical excitations at Nanoscale Tunnel Junctions" **Mehmet Selman TAMER**, Merve ALTAY, Oğuzhan GÜRLÜ, Nanotr7 Conf., Istanbul TR (2011).

- "Photon scanning tunneling microscopy of alloyed gold surfaces" O Gürlü, **Mehmet Selman TAMER**, M Sertkol, R Yilmaz, D Yildiz, ECOSS 29, Edinburg UK (2012)

- "Silicon microsphere based filtering application for nearinfrared optical fiber based telecommunication", Huzeyfe Yılmaz, Ulaş Sabahattin Gökay, **Mehmet Selman Tamer**, Oğuzhan Gürlü, Ali Serpengüzel, International Conference on Optical MEMS & Nanophotonics (2011)

- "Tuning of optical resonances of a microsphere with liquid crystal" Hasan Yilmaz, **Mehmet Selman Tamer**, Oguzhan Gürlü, Ali Serpengüzel, Integrated Photonics: Materials, Devices, and Applications (Proceedings Volume) (2011)